

---

---

# Radars for the Detection and Tracking of Ballistic Missiles, Satellites, and Planets

Melvin L. Stone and Gerald P. Banner

■ This article is an overview of the forty-plus years in which Lincoln Laboratory has been developing and applying radar techniques for the long-range detection and tracking of ballistic missiles, satellites, and planets. This effort has included the development and use of several large radar systems: the AN/FPS-17 radar in Turkey, the Millstone and Haystack radars in Massachusetts, and the Ballistic Missile Early Warning System (BMEWS). The Millstone and Haystack radars have been used to make significant contributions to space science and deep-space satellite tracking. The availability of high-power radars has spurred their application in ionospheric and radar-astronomy studies. The processing techniques developed in support of the astronomical mapping of the Moon and planets provided the foundation for subsequent radar imaging of objects in space. We highlight the radar technology involved and discuss the use of these systems and their legacy.

THE RADAR SYSTEMS DISCUSSED in this article were developed in direct response to significant threats to U.S. national security. These threats included the development of nuclear-armed intercontinental ballistic missiles (ICBMs) and the launching of military satellites in near-earth and, subsequently, deep-space orbits. The complexity and urgency of each threat required a quick response utilizing and extending state-of-the-art radar capabilities. Lincoln Laboratory's successful efforts to develop these radars yielded vital information about the threats. The radars left a legacy of surveillance capability that is still benefiting the United States today. Radar-based studies in astronomy and the ionosphere that utilized this surveillance capability continue to be relevant to science and defense applications.

In the early 1950s, Lincoln Laboratory was developing the Semi-Automatic Ground Environment system (SAGE) in response to the long-range bomber threat from the Soviet Union [1]. Significant ad-

vances had been made in all three of the primary SAGE components: radars, computers, and communications. By the mid-1950s, the prospect of the Soviet Union using ICBMs as well as long-range bombers to deliver thermonuclear warheads became real. The United States needed to confirm the existence of the Soviet ICBM program and monitor its missile tests, which led to the development of the AN/FPS-17 radar. When the missile threat potential had been established, the Ballistic Missile Early Warning System (BMEWS) was developed to warn the United States of a missile attack [2]. Two kinds of UHF radars (surveillance and tracking) comprised the original BMEWS system.

A developmental model of a long-range UHF tracking radar was installed at Millstone Hill in Westford, Massachusetts, to demonstrate the feasibility of advanced Doppler processing, high-power system components, and computerized tracking needed for BMEWS. An adjunct high-power UHF test facility

employed the Millstone transmitter to stress-test the components that were candidates for the operational BMEWS.

The Millstone radar observed missiles fired from Cape Canaveral, Florida, as well as early satellites, and performed pioneering experiments in ionospheric physics and lunar and planetary detection. In the early 1960s, the Millstone radar was converted from a UHF to an L-band system. Both incarnations of the radar proved valuable in defense and scientific applications. Anticipating the need for a high-power facility for communications and space surveillance, the Air Force in the 1960s sponsored the development of Haystack, a versatile facility in Tyngsboro, Massachusetts, that supports radar- and radio-astronomy research and the national need for deep-space surveillance. By the 1970s the Soviets employed deep-space satellite orbits for military use. In response, Lincoln Laboratory applied real-time coherent integration to the detection and tracking of deep-space satellites. The Millstone and Haystack radars continue to operate in the twenty-first century, supporting national space surveillance and scientific missions.

### **Observation of Soviet ICBM Tests with the AN/FPS-17 Radar**

The prospect of a Soviet ICBM raised the possibility of nuclear weapons descending on the United States without warning or defense. This possibility constituted a critical threat to the United States in the mid-1950s and exposed the urgent need to confirm the existence of a Soviet ICBM test program, characterize its capabilities, and monitor its development. William M. Siebert, leading analyses at Lincoln Laboratory from 1954 to 1955, established the possibility that high-power radars could be built to fill this need—and, in fact, were the only feasible technology that could be applied [3]. The result was the expedited construction of the AN/FPS-17 radar in Pirinçlik (originally Diyarbakir), Turkey, chosen because of its proximity to the ballistic missile launch test site at Kapustin Yar in the Soviet Union. Figure 1 shows an artist's conception of the AN/FPS-17 radar facility. The radar was built under Air Force sponsorship with General Electric Company (GE) as primary contractor and, in a highly unusual arrangement due

to the urgency of the need, Lincoln Laboratory as a subcontractor to GE.

Although many of the fundamental concepts used to build air-defense radars applied to the detection and tracking of ballistic missiles, there were significant technical challenges to building a radar for this task. The radar would be hundreds of kilometers from the launch site and would need to observe rockets in flight that were additional hundreds of kilometers away in range. The small target size and the long ranges to the targets required great sensitivity, thereby driving the need for high-power transmitters, a large antenna, and long pulses to maximize average power. However, the use of long continuous-wave (CW) pulses yielded poor range resolution, limiting the accurate characterization of any observed missile tests. A significant contribution by Lincoln Laboratory was the conceptualization and first-ever implementation of a receiver-exciter system that used a phase-coded pulse-compression system to increase the range resolution by a factor of 100 while still using long pulses for maximum energy on target and accurate measurements of the range rate.

The radar was designed around the existing high-power VHF transmitters being produced by GE for domestic television transmission. The tubes used had a center frequency of 198 MHz with a peak power of 1.5 MW. They were operated with 2-msec pulses at a 50-Hz pulse-repetition frequency (PRF), yielding an average power of 150 kW.

The system was designed with a very large antenna to maximize the radar detection range. The resulting antenna reflector was a portion of a paraboloid of revolution almost half an acre in size (175 ft high by 110 ft wide). Lincoln Laboratory designed and directed the construction of the antenna system. The feed consisted of two horizontal rows of feedhorns that formed a pair of azimuth-scanned beams (each scan was approximately 15° wide) at two elevation angles. Lincoln Laboratory also developed a high-power rotary radio-frequency (RF) switch for time-sharing a single transmitter among the feedhorns for continuous azimuth-sector scanning. This switch was an original implementation of a switch in which a noncontacting blade is rotated past a series of output couplers connected to the feedhorns. The phase-

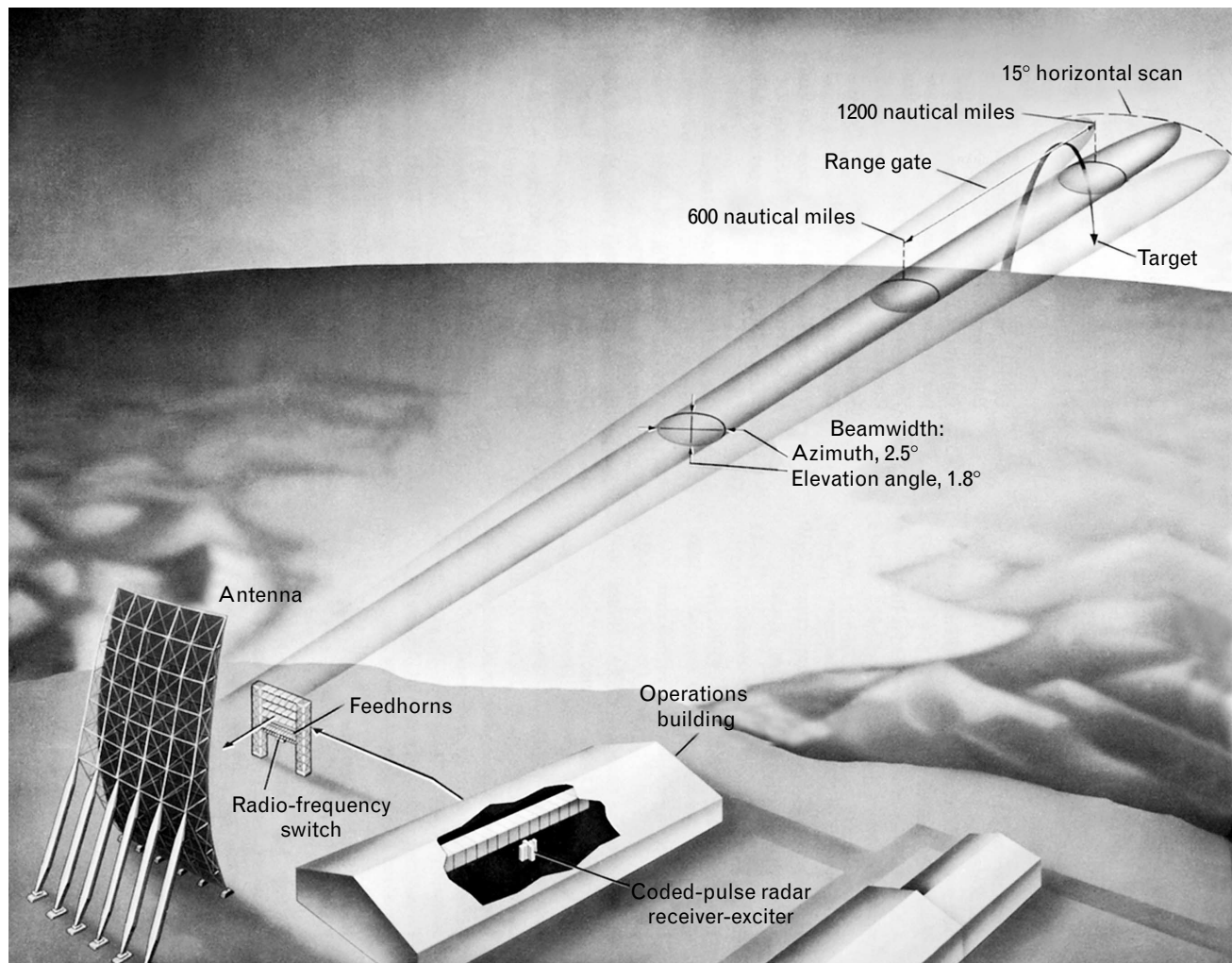


**FIGURE 1.** Artist's conception of the AN/FPS-17 radar facility in Turkey, which was designed and built in the mid-1950s to monitor missile launches from the Soviet Union ballistic missile launch site at Kapustin Yar.

coded pulse-compression system developed by Lincoln Laboratory was a marvel for the mid-1950s [4]. The 2-msec pulse was propagated down a tapped acoustic delay line (approximately 10 m of invar rod) that had 100 taps spaced 20  $\mu$ sec apart. A linear-shift-register pseudo-noise sequence of 1s and 0s determined whether or not the 20- $\mu$ sec subpulses were phase-shifted by 180°. This process was performed at the first intermediate frequency (IF) of 200 kHz before the up-conversion through two more levels to the high-power transmission at 198 MHz. On receive, the process was reversed, yielding a matched filter with the 2-msec pulse compressed to a 20- $\mu$ sec spike, resulting in a much finer range resolution of 3 km [5].

The uncompressed 2-msec pulse was used to ob-

tain a range-rate resolution of 375 m/sec. To achieve this resolution, echo signals from the taps of the delay line were fed through resistive matrices for each resolvable Doppler bin, which weighted the signal to provide quadrature detection. Instead of using a full set of 100 Doppler bins, 18 bins were used to cover the range of expected Doppler returns. The range rate was then calculated from the measured Doppler shift in the targets.

A high-speed 35-mm black-and-white camera recorded the video and status data displayed at the AN/FPS-17 radar. The captured data included such quantities as elapsed time and signal return by Doppler bin, and showed which of the feedhorns had been illuminated. Approximately 240 sec of data could be

recorded. The data-reduction process was manual and cumbersome, but also relatively straightforward.

The successful completion of the AN/FPS-17 in early 1956, fifteen months after the start of the project, remains a remarkable technical achievement that reflects the heroic efforts of dedicated engineers and scientists. The development and implementation of a pulse-compression system contributed significantly to the success of the project.

In 1988, C.E. Cook (Sperry Gyroscope Co.) and Siebert (MIT) shared the IEEE Aerospace and Electronic Systems Society's Pioneer Award for their contributions to the development of pulse-compression techniques for radar signal processing [6]. Phase-coded pulse compression has been widely used in planetary astronomy and for communications with space probes at solar-system ranges.

The Turkey site was the first radar built for tracking at ranges greater than 1000 km, and it gathered much valuable data. Other units were constructed by GE in Texas for observing domestic test flights over the White Sands Missile Range, New Mexico, and Shemya, Alaska, to observe the later stages of Soviet ICBM tests.

### The Ballistic Missile Early Warning System

While the AN/FPS-17 was being constructed to confirm and characterize Soviet ICBM capabilities, the development of a system for reliable, timely warning of ICBM attacks against the United States became an important national priority as a vital link in the Cold War concept of mutually assured destruction. Lincoln Laboratory played a major role in the design and development of the Ballistic Missile Early Warning System (BMEWS), which provided the necessary warning time for counterstrike action to be launched. For the interesting story behind one high-level threat warning issued by BMEWS, see the sidebar entitled "False Alarm!"

As a result of both experimental and systems studies [7], Lincoln Laboratory recommended the basic BMEWS configuration that was adopted by the Air Force. It consisted of three operational sites in Thule, Greenland; Clear, Alaska; and Fylingdales Moor, United Kingdom, with two basic types of radars—surveillance/detection radars scanning in azimuth at

two fixed elevation angles and pencil-beam tracking radars—as well as real-time data communications to the North American Air Defense Command (NORAD) in Colorado Springs, Colorado. Figure 2 shows three AN/FPS-50 BMEWS surveillance radars in Clear, Alaska. System requirements included long-range detection of missiles out to 4800-km range to provide warning, target-threat characterization, accurate tracking for impact-point estimation, and communications to inform the command center for formulating counterstrike decisions.

The surveillance radar operated at UHF (440 MHz) and included a parabolic-torus antenna with an organ-pipe-scanner feed, a high-power transmitter, a receiver with a Doppler filter bank, a data-processing computer bank, and a communications interface. The prototype for the radar, designated the AN/FPS-50, was built by GE in Trinidad, where it was used to support missile tests launched from the U.S. Atlantic Missile Range in Cape Canaveral. Lincoln Laboratory's contributions were significant. They included the design and development of the high-power organ-pipe feed (using a rotating horn to illuminate a sequence of feeds on the focal arc of the torus) [8], Doppler filter banks, algorithms for target-threat characterization, and the specification and testing of many other radar components.

The pencil-beam tracking-radar component of the BMEWS also operated at UHF. Lincoln Laboratory



**FIGURE 2.** Three Ballistic Missile Early Warning System (BMEWS) AN/FPS-50 surveillance radars at Clear, Alaska. The parabolic-torus antenna reflector of an AN/FPS-50 radar was approximately the size of a football field.

---

---

## FALSE ALARM!

THE BALLISTIC MISSILE Early Warning System (BMEWS) performed well for over three decades. However, during the Initial Operating Capability (IOC) phase in the fall of 1960, it generated a high-level threat warning report that was an incident of great concern to the Defense Command Staff.

On 6 September 1960, the Thule, Greenland, BMEWS site began generating warning reports at the lowest threat level that rapidly escalated up to the maximum level. It automatically sent a series of messages warning of an impending missile attack to the North American Air Defense Command (NORAD) in Colorado Springs, Colorado. Before alerts could be sent to the President and dispatched to the Strate-

gic Air Command bombers, the alerts had to be validated by means of a direct telephone conversation between Command Center personnel and the radar site. An Air Force captain at the site asked for time to perform a check on the radar because he believed it was malfunctioning. He temporarily turned off the transmitter in the sector that was generating the alarms and noted that the echoes ceased. He correctly inferred that the echoes were caused by reflections from the Moon; a hostile missile threat did not exist. The great power and aperture of the BMEWS radar allowed it to detect reflections from the Moon, which was 384,400 km away.

In December 1960, a Lincoln Laboratory team was sent to Thule to investigate a number of

issues related to the IOC, including the Moon echoes. The BMEWS contractor, Radio Corporation of America, had proposed a low-perigee test that eliminated most but not all of the false-alarm conditions attributed to Moon echoes. A member of the Lincoln Laboratory team recognized that simply changing the operating frequency of the radar about every two seconds (less than the round-trip Earth-Moon travel time) could unconditionally eliminate the Moon echoes. This recommendation was presented to the Commander of the North American Air Defense Command on 20 January 1961 and implemented in the radar in conjunction with other improvements. The Moon ceased to be a source of false alarms.

successfully developed the required technology and it was demonstrated at the Laboratory's Millstone Hill radar facility. The Millstone radar served as a development model for RCA's AN/FPS-49, AN/FPS-49A, and AN/FPS-92 radars, all of which were used in the BMEWS. The first site at Thule, Greenland, became operational in 1960 with four AN/FPS-50 surveillance radars, all powered by big UHF klystrons. An AN/FPS-49 tracker was added later.

The installation stretched for over 1.4 mi and used over 10 miles of 21-in-wide waveguide. The second site, at Fylingdales Moor, United Kingdom, had three AN/FPS-49A trackers to provide intermediate-range-missile warning for the United Kingdom and long-range-missile warning for North America. The third

site at Clear, Alaska, had three AN/FPS-50s and an AN/FPS-92. The twelve large UHF radars of the original BMEWS performed their critical missile-warning functions as well as satellite-surveillance and tracking functions with extremely high reliability for close to thirty years. In time it became possible to replace them with UHF solid-state phased-array radars. The first of these new radars came online at the Thule BMEWS site in 1987; the last came online at Clear in 2001. These new radars use the same transmit/receive modules and array-element design as the four UHF Precision Acquisition of Vehicle Entry Phased Array Warning System (PAVE PAWS) radars (AN/FPS-115, later AN/FPS-123) that were built within the continental United States to provide warning of sub-



**FIGURE 3.** The UHF Millstone Hill radar with its reflector and scanning feed, circa 1958. Located in Westford, Massachusetts, the Millstone system included an 84-ft paraboloidal reflector and conical feed mounted on an elevation-angle-over-azimuth pedestal and a klystron transmitter operating at UHF with 1-MW peak and 60-kW average power.

marine-launched ballistic missiles. The upgraded BMEWS remains an important component of our national security system.

### The Millstone Hill UHF and L-Band Radars

In 1956, even before the BMEWS design concept was completed, the Laboratory began construction of the Millstone Hill radar, shown in Figure 3, as an experimental system to demonstrate the feasibility of accurately tracking ballistic missiles at long ranges. The radar site was Millstone Hill on 1100 acres of property owned by MIT in Westford, Massachusetts—about 20 miles northwest of the main Lincoln Laboratory facilities at Hanscom Air Force Base in

Lexington, Massachusetts [9]. The specifications for the Millstone system included an 84-ft paraboloidal reflector and conical scanning feed mounted on an elevation-angle-over-azimuth pedestal, a klystron transmitter operating at UHF with 1-MW peak and 60-kW average power, a 2-msec-pulse radiated signal, a Doppler filter bank, and a solid state computer for a calculation of the missile trajectory and impact point.

All of the RF components existed generally at shorter wavelengths and two orders of magnitude less operating power. Thus, although Millstone required no fundamental hardware technology breakthroughs, there were significant challenges in scaling the components to operate in the UHF band (440 MHz) at the required high power levels and incorporating them with the rotating conical-scanning feedhorn and the large agile antenna atop its 85-ft pedestal [10]. At the time, Herbert G. Weiss, the father of Millstone, often said, “All we needed was about a 50-dB gain in sensitivity.” (Long-range UHF air-defense radars detected 10-m<sup>2</sup> aircraft at 400 km; Millstone was to detect 1-m<sup>2</sup> targets at over 4800 km.)

Among the critical UHF components successfully developed at Millstone were the turnstile junction that provided polarization adjustment, the conical-scanning feedhorn used to develop angle-tracking error signals, the rotating joints used on the two axes of the antenna mount, and the duplexer used to protect the receiver during the high-power transmitted pulses. A UHF maser was employed in radar-astronomy observations.

The receiver was a coherent superheterodyne unit that was followed by a coherent crystal-filter bank. Two receivers used 125 Doppler filters attached to each of them. A “greatest of” circuit examined the outputs of the filter bank to identify the filter having the largest signal. This Doppler filter-bank scheme, developed by Aaron A. Galvin, was the same one mentioned above for the AN/FPS-50 [11]. At Millstone, the amplitude, range, angular position of the target, and filter number (corresponding to Doppler frequency and thus range rate) were transmitted to the input of the CG-24 computer, where trajectory estimates were made.

Figure 4 shows the CG-24 computer, which Lincoln Laboratory designed and built for Millstone as



**FIGURE 4.** Original Millstone site CG-24 computer, circa 1960. All functions performed by the CG-24, which took up an entire room, could now be performed by one of today's desktop computers.

the first entirely solid state computer used for real-time processing of radar data [12]. It was installed at the radar in 1958 for radar tracking. The CG-24 computer was a major factor in the development of digital data-processing techniques that were fundamental in the evolution of modern radars. The CG-24 was dedicated to the tasks of real-time control of the antenna and calculation of the trajectories and impact points of threat missiles.

In the absence of threat missiles, the radar and computer were tested against rocket launches from Cape Canaveral. In an original work, Irwin I. Shapiro developed the theory for predicting ballistic missile trajectories from radar observations [13].

The Millstone radar successfully demonstrated the feasibility of detecting ballistic missiles at a range of a few thousand kilometers [9, 14]. This achievement helped advance the construction of the BMEWS, with Millstone as the model for the radars installed in Thule (AN/FPS-49), Clear (AN/FPS-92), and Fylingdales Moor (AN/FPS-49A). As mentioned above, the transmitter, receiver, and Doppler filter bank of the BMEWS surveillance radar were patterned after their Millstone counterparts. (An IBM commercial solid state computer was used for the post-detection processing.) Millstone also was the model for a radar built for NASA at Wallops Island, Virginia. Full-scale models of Millstone were installed

at the Air Force downrange tracking station in Trinidad and the Prince Albert Radar Laboratory in Saskatchewan, Canada.

The Trinidad radar supported the Atlantic Missile Range testing and, in the 1960s, provided an operational warning capability for detecting submarine-launched missiles in the Caribbean. The Prince Albert Radar Laboratory system, shown in Figure 5, was employed by the Canadian Defence Research Establishment for study of the aurora and the development of satellite-tracking techniques.

Another major contribution by Lincoln Laboratory was the use of Millstone to develop a fundamental understanding of several important environmental challenges facing the BMEWS. These challenges included the measurement of UHF propagation effects in the ionosphere, the impact of refraction close to the horizon, the effect of Faraday rotation on polarization, and the impact of backscatter from meteors and the aurora on the detection performance of the radar and its false-alarm rate [15–17]. The Laboratory also developed algorithms for use in processing BMEWS data to provide the requisite warning of an impending missile attack.



**FIGURE 5.** Prince Albert Radar Laboratory, Saskatchewan, Canada. The radar is a twin of the UHF Millstone radar shown in Figure 3. During the dedication ceremony on 6 June 1959, President Eisenhower made the first communication between heads of state by using a passive satellite reflector, the Moon, when he greeted Canadian Prime Minister Diefenbaker via a prerecorded message. The Millstone radar site, equipped with a single-sideband transmitter, broadcast the message.

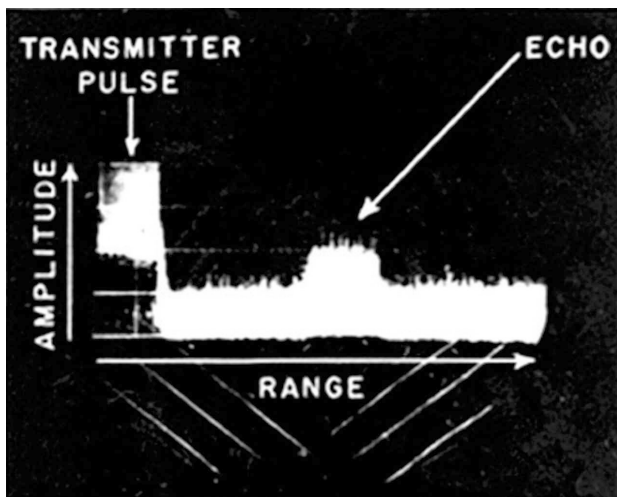


**FIGURE 6.** Detection in 1957 by Millstone UHF radar of the first Soviet satellite, *Sputnik I*. The display shows amplitude versus range of the transmitted pulse and the echo.

Even before its completion—with the high-power transmitter, conical-scan tracking system, and CG-24 not yet fully developed—Millstone was used in an unexpected way when the Soviet Union surprised the world by launching *Sputnik I* on 4 October 1957. By the next day, Millstone had successfully detected *Sputnik I* [18]. Figure 6 shows the first detection of an artificial Earth satellite by active radar. Many sites detected the radiated signal from *Sputnik I*, but the Millstone activity was unique because it transmitted RF signals from the transmitter-driver stage and detected the energy reflected from the satellite back to the radar. The receive signals were displayed on an A-scope. Thus both the space age and the U.S. space-surveillance system were born.

The Millstone UHF system was completed in 1958. Since the early 1960s, the tracking of satellites has been Millstone's primary role in supporting defense interests. In 1960, its peak power was increased from 1 MW to 2.5 MW (with a corresponding increase in average power to 150 kW). By 1962, the BMEWS was complete and the Millstone radar was reconfigured to operate at its present L-band (1295 MHz) frequency.

John V. Evans continued to use the original UHF system for ionospheric and upper-atmosphere studies. A 220-ft zenith-pointing antenna was installed in 1963 to support vertical sounding measurements. In

1977, a 150-ft, fully steerable antenna was installed to study horizontal motion in the ionosphere [19]. Both of these antennas are shown in Figure 7.

In September 1994 the 104-in-diameter azimuth bearing atop the Millstone radar's antenna pedestal failed for the first time since it had been erected in 1957. A spare bearing was on hand, but the radar was to be out of commission for six weeks to replace the bearing. To cover this gap in radar support to the U.S. Space Command, a descendant of the original Millstone UHF transmitter and the nearby 150-ft-diameter steerable antenna were partially diverted from their scientific tasks and brought into service for satellite tracking. The UHF radar's antenna was less accurate in angle than that of the L-band Millstone, but the stopgap radar made a useful contribution.

The conversion of Millstone to L-band represented several significant advances in radar technology [20]. (The original antenna was removed and shipped to Pirinlik, Turkey, where it was used as part of the UHF system there for over twenty years.) A new paraboloidal antenna with a finer mesh matched to the shorter L-band wavelength was placed atop the



**FIGURE 7.** UHF antennas for ionospheric measurements at Millstone Hill. The fixed 220-ft zenith-pointing antenna (left) was installed in 1963 and the steerable 150-ft-diameter antenna (right) was installed in 1977.

85-ft pedestal. The new system employed a Cassegrainian feed in place of the rotating conical-scan feed used at UHF. A two-tube klystron transmitter system provided over 3 MW of peak power and 120 kW of average power. Nominal operating parameters included a 1-msec pulse and a 40-Hz PRF. The maximum bandwidth was 8 MHz, yielding a range resolution of approximately 30 m. The transmitted wave was right-hand circularly polarized. For reception, both the principal (left circular) and orthogonal (right circular) channels were processed as well as the two angle-error channels. The unique features of the Millstone L-band radar included parametric-amplifier receivers (since replaced by low-noise solid state amplifiers), a set of L-band “pancake” low-power rotating joints, a slip-ring system allowing continuous motion without cable wrap, and a twelve-horn monopulse feed. Figure 8 shows how the feed provided optimum illumination of the reflector to form the sum-channel main beam plus azimuth and elevation-angle-difference channel beams required for generating angle-tracking signals [21, 22].

**Haystack**

The Air Force and Lincoln Laboratory recognized the need for a flexible facility to develop and evaluate radar and communications technology. Under the leadership of Weiss [23, 24] the Haystack 120-ft antenna and a very high-power transmitter were assembled in a 150-ft radome located about half a mile down the road from Millstone. The Cassegrainian antenna included many innovative design features. Interchangeable boxes, installed behind the Cassegrainian focus, allowed for the exchange of equipment for experiments ranging from high-power radar and communications to passive radiometry.

The antenna is housed in a metal space-frame radome designed to withstand 130-mph winds. The metal space frame occupies approximately 6% of the spherical surface of the radome. The blocking action of the space frame results in a loss of approximately 11% of the effective aperture while providing a wind-free environment. When constructed, the space frame supported 0.032-in-thick fiberglass panels having a lost tangent of approximately 0.01°. In a range of frequencies from 1 to 10 GHz, the loss attributable to

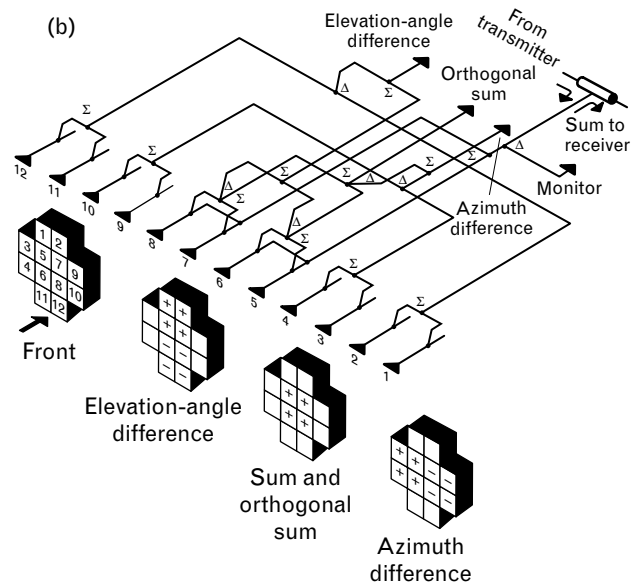
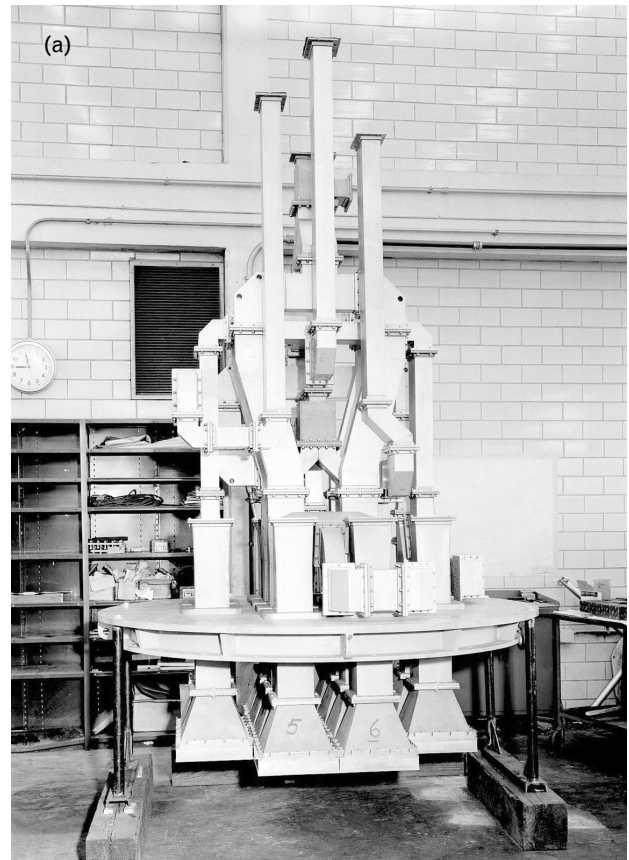


**FIGURE 8.** (a) The twelve-horn L-band monopulse feed. Replacing the conical-scanning UHF feed, it provides optimum illumination of the reflector to form the two main-sum beams and the azimuth-difference and elevation-angle-difference beams required for generating angle-tracking signals. (b) The excitation of the twelve feedhorns for each mode.



**FIGURE 9.** The Haystack antenna panels and multiple radiometer feedhorns, circa 1994. The feedhorns are mounted on a cylindrical support at the center of the paraboloidal reflector.

the space frame is 1.1 dB. The dielectric constant of the panels is approximately 4, resulting in an increasing reflection at frequencies above 8 GHz. As originally designed the radome provided a useful capability for frequencies up to 15 GHz.

Mechanically, the antenna represented a *tour de force* in structural design and analysis, state-of-the-art manufacture of precision structures, surface alignment, contour determination [25], and drive system control [26]. When the antenna, shown in Figure 9, was constructed in the 1960s there were no existing digital-design-and-drafting tools or methodologies for estimating the performance of such a complex structure. A rigorous mathematical model that supported the analysis of 4000 joints was developed and confirmed by measuring the deflection on a 1/15-scale structural model that was subjected to a variety of loading conditions. (The MIT Civil Engineering Department developed a program called STAIR in 1957 to handle large truss structures having only 60 pin-ended joints.) The Haystack antenna analyses and modeling validated the analyses done by both MIT and North American Aviation, the contractor for the fabrication and installation of the antenna. An IBM Frame Analysis (FRAN), which was developed later, supported the analysis of rigid joints. Thermal analyses indicated that the air temperature in the ra-

dome would have to be controlled with a gradient of less than 10°C across the 120-ft diameter to maintain the distortion of the reflector to within approximately  $\pm 0.010$  in [27]. A heating and blower system was installed to maintain the temperature.

Figure 10 shows the entire Haystack antenna structure, which weighs approximately 400,000 lb. It is supported on a hydrostatic bearing consisting of 24 individual bearing pads that maintain a clearance of  $\sim 0.005$  in when operating with a pressure of less than 1000 psi [28]. The bearing is essentially frictionless. The yoke and elevation-angle bearings support the re-

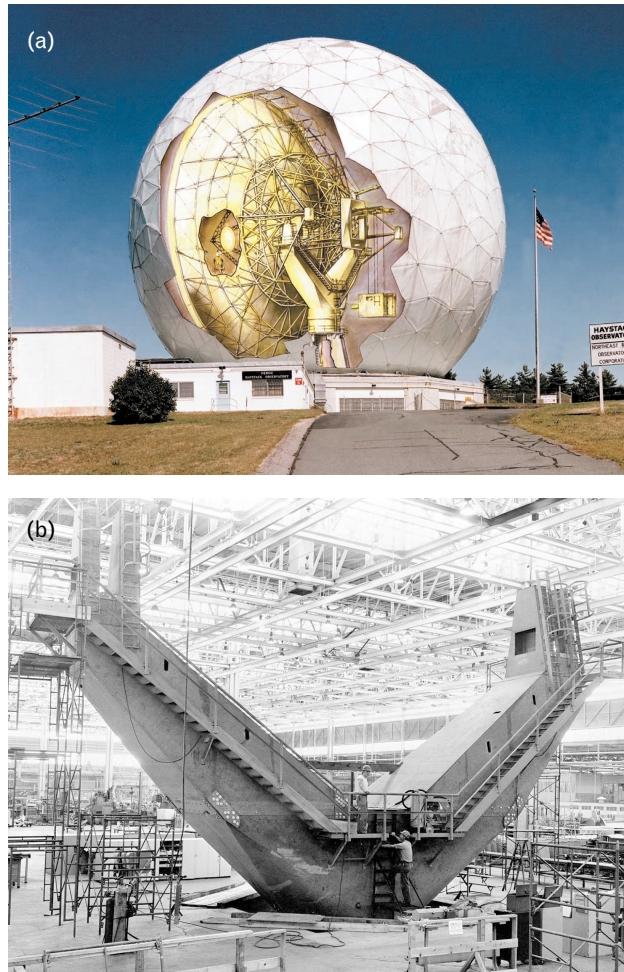


**FIGURE 10.** (a) Cutaway illustration of Haystack. A 150-ft radome encloses the 120-ft paraboloidal reflector, its bicycle-wheel-like support structure, the removable equipment shelter, and the yoke assembly. (b) A photograph of the azimuth and elevation-angle yoke, conveying the scale. Note the size relative to the human figures standing at the base of the yoke.

flector and back structure of the antenna as well as the interchangeable equipment shelter. Ninety-six shaped panels manufactured with a root-mean-square (rms) surface tolerance of 0.010 in are attached to a 60-ft-diameter splice ring and supported from a bicycle-wheel-like structure. The antenna was designed to point to and track both nearby satellites and the positions of celestial objects. A then state-of-the-art computer-controlled hydraulic servo system drove the antenna. A 30-bit computer provided the requisite accuracy for tracking astronomical objects.

The 120-ft reflector was specified to have a surface tolerance of 0.075 in to meet the original design goal for operation at 10 GHz. Owing to the existence of the rigid, complex backup structure, a gravity-compensating counterweight, a manual set of adjustments, and a novel statistically based rigging technique, the reflector was readjusted to operate at 15 GHz about two years after it was initially installed.

A six-year effort, started in 1986, resulted in the upgrading of the Haystack radio telescope for astronomical operation at 85-to-115 GHz. The National Science Foundation supported the upgrading program that was performed by the Northeast Radio Observatory Corporation (NEROC) and the Haystack Observatory staff and its supporting contractors. Richard P. Ingalls led a team of sixteen scientists and engineers in implementing major enhancements to the 120-ft reflector, the hyperboloidal subreflector, the thermal compensation of the back structure and radome, and the technique for mapping surface deviations [29]. The upgrade took place in two stages: the first three-year effort increased the system's aperture efficiency to 25% at 35 GHz; the next three years extended the frequency coverage to the 85-to-115-GHz range. The first phase comprised the installation of new membrane material on the radome, the upgrading of the thermal control of the entire surface, and a readjustment of the surface of the paraboloidal reflector to attain a 0.020-in (450- $\mu\text{m}$ ) rms tolerance. Attaining the second-phase goal required further improving the thermal compensation, adjusting the paraboloidal surface to a 0.010-in (210- $\mu\text{m}$ ) rms tolerance, and installing a deformable subreflector [30, 31].

One of the major limitations of extending the op-

erating frequency range of the Haystack antenna was the existing thermal lag of a 60-ft-diameter splice ring that interconnected the inner and outer sets of the 30-ft-radial-length panels. A bidirectional thermo-electrical control system was installed on the splice plate to cause its temperature to track that of its neighboring panels. In addition, electric heating and chilled-water cooling were used to quickly adjust the temperature when the antenna changed elevation-angle position rapidly.

Extensive finite-element analyses were made of all the components of the Haystack antenna. A finite-element model of the paraboloidal surface was constructed to facilitate the setting, both statically and dynamically, of the many adjustments of the primary and secondary reflector surfaces.

Measurements of the 120-ft paraboloid were performed by microwave holography employing Very Long Baseline Interferometry (VLBI) techniques. The Haystack antenna and a reference antenna received signals from a geostationary communications satellite operating in the 12-GHz band. They were correlated by the Haystack VLBI processor operating in a real-time mode. These measurements involved a comprehensive elimination of the effects of the space-frame radome that both blocks and diffracts the satellite signals, causing distortions of the mapping of the surface of the antenna. The process mapped the paraboloidal surface with an estimated accuracy of 100  $\mu\text{m}$  in equivalent surface deviation [32].

A precision thermal-control system was added for compensation of the gravitational deformation of the reflector. Because not all of the deformation could be compensated thermally, a deformable, fiber-reinforced plastic hyperboloidal subreflector was developed to correct for gravity and astigmatic deformations of the back structure of the 120-ft reflector.

The upgrading program achieved its objectives of a 17-arcsec beamwidth (8.24  $\mu\text{rad}$ ) and 15% efficiency at 115 GHz. Blind pointing of the antenna within 4 arcsec and tracking within 2 arcsec was realized.

In addition to the antenna system, high-power radar components were also improved. In the 1960s the development of a system for use in planetary astronomy [33] significantly advanced the state of the art of X-band high-power technology. A number of

firsts were achieved, including the development of a 500-kW CW transmitter with its associated high-power waveguide components, an ephemeris-controlled frequency and range-tracking system, a helium-cooled maser receiver preamplifier, and a digital monitoring system to prevent damage of the high-power components. For lunar measurements the system was equipped with a pulse modulator and appropriate transmit/receive switch to accommodate the ~2-sec radar transit time.

A wideband radar system known as the Haystack Long Range Imaging Radar (LRIR) was assembled in 1977 to support the observation of satellites. That radar continues to operate to this day. (For more information on this topic, see the article entitled “Wideband Radar for Ballistic Missile Defense and Range-Doppler Imaging of Satellites,” by William W. Camp et al., in this issue.)

In the early 1990s, increased interest in the wideband imaging capability of Haystack led to the development of the Haystack Auxiliary Radar (HAX). By utilizing a 2-GHz bandwidth centered at 16.667 GHz and a refurbished 40-ft antenna, HAX was able to share much of the signal and data-processing systems of the LRIR and thus provide full-time availability for the imaging of satellites. The sharing of the processing systems reduced development and operations costs under the constraint that only HAX or the LRIR could be operational at one time.

### **Radar Astronomy and Space Science**

In addition to defense-related activities, the Millstone radar and subsequently Haystack contributed significantly to the fields of ionospheric, lunar, and planetary science. Important theoretical contributions were made in the early 1960s: Robert Price and Paul E. Green described radar-astronomy signal-processing techniques [34] and Green described the use of range-Doppler imaging in radar astronomy [35]. Evans and Tor Hagfors edited a comprehensive book summarizing theory, instrumentation, and observations in radar astronomy through the mid-1960s [36].

Pioneering planetary radar observations were made in the late 1950s and early 1960s with the Millstone radar. The more powerful Haystack radar played a

prominent role during the 1960s in refining the knowledge of the solar system and in the mapping of the Moon. Gordon H. Pettengill led efforts to observe the reflection characteristics and mapping of the Moon and planets noted herein.

An aeronomy program commenced in 1959 with the first observation of Thomson scattering in the ionosphere. This work was relevant to the scientific community and played a key role in studies related to ballistic missile defense.

### *Ionospheric Studies*

The Thomson-scatter observation, made in 1959 by Victor C. Pineo [37, 38], was the world's first confirmation of J.J. Thomson's physical theory on the incoherent scattering of radio waves by electrons in the ionosphere. W.E. Gordon postulated the existence of Thomson scattering in the ionosphere [39]. From 1963 to 1982, the Millstone facility performed and documented measurements of ionospheric properties, including dynamic effects [40, 41], electron densities, and electron and ion temperatures [42–44]. In 1977, installation of a UHF 150-ft fully steerable antenna was completed to support investigation of the mid-latitude ionosphere that rotates with the Earth and the auroral ionosphere that does not [45]. Evans led the synoptic ionospheric research by using the 220-ft zenith-pointing fixed antenna and the steerable 150-ft paraboloidal antenna, both shown in Figure 7. He published over fifty journal articles covering these activities.

From 1969 to 1973, the Millstone facility was engaged in a propagation study to characterize the impact of ionospheric effects on precision measurements required for ballistic missile defense. The U.S. Army Ballistic Missile Defense Agency and the U.S. Army SAFEGUARD System Command sponsored the program, conducted jointly with Bell Telephone Laboratories. Satellites of the U.S. Navy Navigation Satellite System (the predecessor of the Global Positioning System, or GPS) were tracked simultaneously by using the UHF navigation signals radiated by the satellites and their L-band radar echoes to observe and measure the effects of the ionosphere refraction. Bell Telephone Laboratories employed these measurements and the Thomson-scattering measurements in

their development of propagation models appropriate to ballistic missile defense [46, 47].

The object of the study was to determine the angular bias refraction of UHF beacon signals as they passed through the ionosphere. The bias was accurately determined by averaging many daytime satellite passes. Good agreement was found among predictions based on ray-tracing studies performed by Bell Telephone Laboratories, incoherent scattered electron-density profiles, and real-time measurements of the electron content along the line of sight to the satellite that were obtained by differential-Doppler observations.

Signal-amplitude fluctuations caused by the ionospheric-density irregularities were observed in the auroral zone. Angular scintillation above the threshold of detectability occurred less frequently than the fluctuations. Considerable information gathered on the occurrence of scintillation as a function of the time of day and geomagnetic activity was summarized in the form of a simple model.

The most serious source of angular scintillation in the apparent position of the UHF satellites was the existence of ionospheric waves known as traveling ionospheric disturbances (TID). Two classes of waves were identified. TIDs with wavelengths in the 25-to-50-km range were common. They gave rise to fluctuations in the apparent elevation angle of the target with periods of less than 10 sec and amplitudes as large as 80 millideg (peak to peak). TIDs with wavelengths in the 100-to-1000-km range were less common but could be readily recognized by their clear signature in the differential-Doppler records. They produce somewhat smaller fluctuations in the apparent elevation angle [41].

Lincoln Laboratory made extensive modifications to the Millstone Hill radar facility to accomplish the above measurements. To support the simultaneous use of the Millstone antenna at two frequencies, Lincoln Laboratory and Philco-Ford developed a frequency-selective subreflector (FSS) [48, 49]. It employed both the Cassegrainian and Newtonian foci of the Millstone antenna and was reflective at L-band and transparent at UHF frequencies. Figure 11 shows the Newtonian/Cassegrainian geometry of the FSS.

The unit consisted of a hyperboloidal surface of

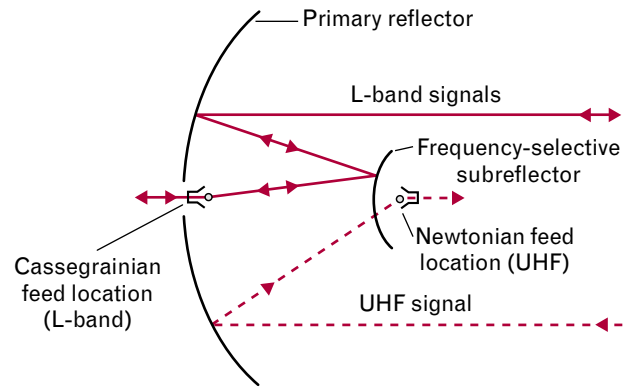


**FIGURE 11.** Newtonian/Cassegrainian geometry of the frequency-selective subreflector (FSS). This sketch shows the relative location of the two feeds with respect to the FSS, which is transparent to low-frequency (UHF) signals and reflective to high-frequency (L-band) signals.

crossed dipoles that reflected both linearly and circularly polarized L-band signals to the feed at the Cassegrainian focus and transmitted UHF signals to a monopulse feed at the Newtonian focus. Figure 12 shows a photograph of the FSS array of L-band crossed-dipole elements mounted on a low-loss, plastic hyperboloidal substrate. The FSS was the progenitor of a two-layer unit that was developed later for use at VHF and UHF on the very high-power Advanced Research Projects Agency (ARPA) Long Range Track-



**FIGURE 12.** The FSS used for the U.S. Army SAFEGUARD System Command propagation study, comprising an array of L-band crossed-dipole elements mounted on a low-loss, plastic, hyperboloidal substrate. The loss in antenna gain at L-band was less than 0.2 dB and was negligible at UHF.

ing and Instrumentation Radar (ALTAIR) radar at the Kiernan Reentry Measurements Site (KREMS). These modifications represented the first use of an FSS in radar having over 100 kW average power.

A study of auroral radar clutter at 1.2 GHz was conducted in conjunction with the satellite particle measurements and airborne optical observations [50]. These observations showed that the evening and morning echoes observed at Millstone are from regions of diffuse proton precipitation lying toward the equator of the main visible auroral arc. No significant tracking perturbations were uncovered that appeared to be associated with the appearance of auroral returns along the line of sight to the satellite.

A comparison of the estimated total electron content of the first 1000 km of ionosphere made by the Millstone incoherent-scatter radar system with an estimate based on GPS measurements made out to a range of approximately 19,000 km showed a significant difference between results obtained by the two measuring techniques. From this comparison it was concluded that at times a significant portion of the total electron content comes from altitudes above 800 km [51, 52].

#### *Radar-Astronomy Studies*

The large power-aperture products and digital signal processing capabilities of Millstone and Haystack allowed researchers to observe the Moon and planets. Commencing in the 1950s scientists at Lincoln Laboratory made significant contributions to radar astronomy [53], including measurements of the Moon [54–57] and Venus [58, 59]. This work continued through the 1960s with the L-band Millstone radar. Beginning operation in 1964, the more powerful Haystack extended the scope of lunar and planetary radar observations to include topographic mapping of the Moon [60, 61], characterization of the topography of Mars [62, 63], Venus, and Mercury, and detection of the asteroids Icarus [64] and Toutartis [65].

Several independent groups from the United States and the United Kingdom reported radar echoes from Venus in the spring of 1961. One of these groups was the Lincoln Laboratory team using the Millstone UHF radar [66]. Earlier Laboratory reports on the detection of radar echoes from Venus were not cor-

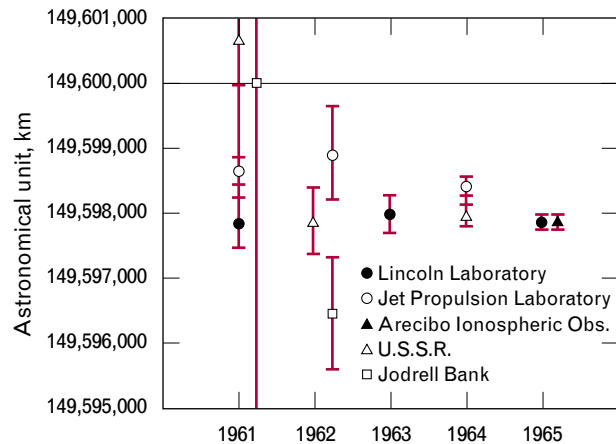


**FIGURE 13.** Radar determinations of the astronomical unit, 1961 through 1965. The most recent determinations by the Arecibo Observatory in Puerto Rico and by Lincoln Laboratory are consistent with the 1965 value but several orders of magnitude more precise. (Adapted from Reference 68.)

roborated and were subsequently judged false [58].

Lincoln Laboratory achieved significant solar system measurements, including the refinement of the estimate of the astronomical unit [59, 67], the establishment of the rotational motion of Venus (243-day period with retrograde motion) [68], the establishment of the radius of the planet, and a radar cross section indicating that Venus is much less porous (i.e., more like solid rock) than the Moon, with a thinner layer of “topsoil” [66]. Similarly, Haystack radar reflections from both Mercury and Mars [62, 63, 69] were instrumental in helping Lincoln Laboratory and the rest of the scientific community analyze the properties of these two planets [68]. Figure 13 shows the radar determinations of the astronomical unit from several laboratories through 1995.

Shapiro proposed employing Haystack to perform time-of-flight measurements to the planets Venus and Mercury as they orbited the Sun to measure the effect suggested by Einstein’s general theory of relativity [70, 71]. The thrust of this fourth test of general relativity was to isolate general relativistic effects from classical mechanical effects. Relativity entered into the experiment in two ways: the anomalous advance of the planetary perihelia (the perihelion is the point in a planet’s orbit where it is closest to the Sun) and in the general relativistic slowing down of interplanetary

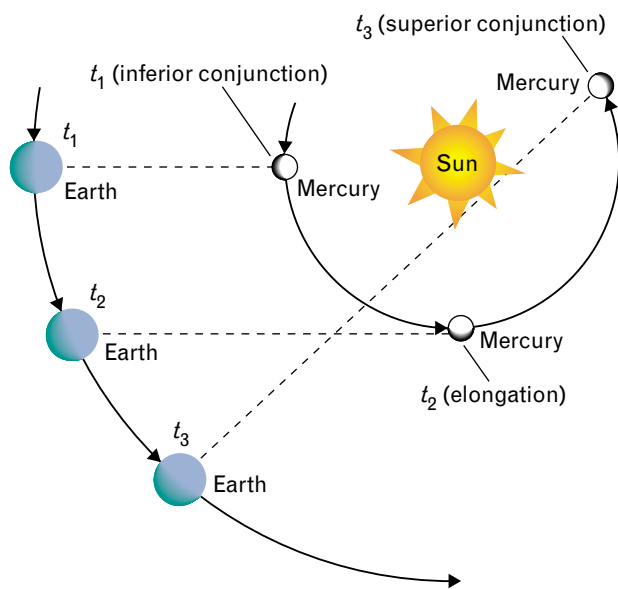


**FIGURE 14.** Plan view of the orbits of Mercury and Earth showing the positions of the planets relevant to the radar observations for the fourth test of Einstein's general theory of relativity. This theory predicts that radar waves traveling to and reflecting off Mercury are slowed down by the gravitational effect of the Sun. The effect would be most pronounced at the time of superior conjunction, when the radar waves pass closest to the Sun. (Adapted from Reference 68.)

radar signals that pass near a massive body. Accurate estimates of the radius and the mass of the planets Mercury, Venus, and Mars, the Earth-Moon mass ratio, and the astronomical unit were obtained by processing the radar measurements along with optical observations. Once the planetary orbits had been precisely determined, measurements of the round-trip transit time to Mercury as it passed behind the Sun provided the data from which the slowing down of the signal could be determined. Figure 14 shows the positions of Earth and Mercury relevant to the fourth test of Einstein's general theory of relativity. Figure 15 shows the slowing down of radar signals due to general relativistic effects.

The radar observations were coupled in iterative analyses with extensive optical observations to refine various parameters of the solar system [67]. The analyses took advantage of the several orders of magnitude improved relative accuracy attained by the radar over the best optical techniques then available for describing the solar system [67].

The fourth test of general relativity presented a formidable challenge in accurately determining solar-system parameters, particularly the interplanetary distances and planetary motions, and in the radar technology needed for accurately measuring the range and Doppler shifts of targets at ranges on the order of 100 million miles.

Major enhancements were made to the radar transmitter/receiver capability and to precision frequency and time control. The use of the ephemeris control in scheduling of pointing the antenna, as well as range sampling and Doppler-shift compensation essential to the fourth test of general relativity, exemplified the technology that was later applied to deep-space satellite observations. Owing to the large transit time, the antenna position had to lead the planet's position in the direction of the planet during the receiving interval.

An atomic hydrogen frequency standard was used for both time and frequency determination. The high Doppler shift (e.g.,  $\pm 4$  MHz at 8 GHz when observing Mercury) made it necessary to use predictive expansion/compression of the sampling interval of the received signal and to track the coherent reference oscillator of the superheterodyne receiver. Doppler predictions were based on an ephemeris that increased in accuracy during the course of the experiment. The reference oscillator was tracked with an rms accuracy

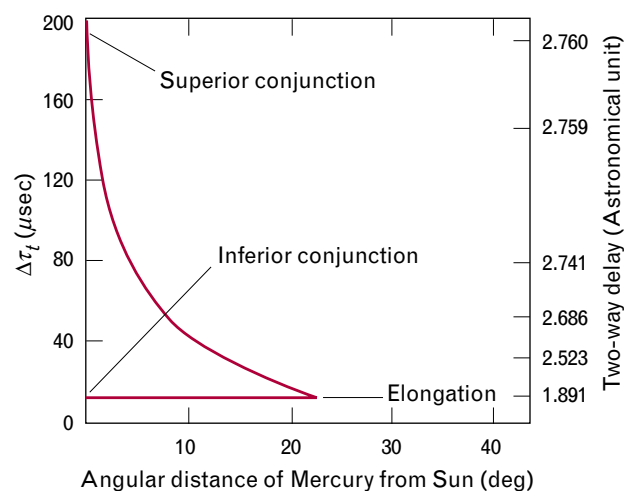


**FIGURE 15.** Contribution of relativistic effects to time delays of radar signals between Earth and Mercury. The time delay is greatest at superior conjunction, when the radar signals pass closest to the Sun. (Adapted from Reference 68.)

of 0.1 Hz and a precision of 0.01 Hz. The time-base expansion/contraction was adjusted proportionally to the Doppler shift. Coherent integration was performed over an interval of approximately  $10^3$  seconds. The coherent data sets obtained were incoherently integrated for up to fourteen hours. Measurements of radar echoes made when the paths of Venus and Mercury were nearly tangential to the Sun allowed scientists to estimate the relativistic delay predicted by Einstein's general theory of relativity.

Millstone and later Haystack supported pioneering radio-astronomy work performed by MIT students and faculty during the 1960s and 1970s. This work came under the aegis of the NEROC in 1967.

Working with a National Science Foundation grant to the MIT Research Laboratory of Electronics (RLE) under the late Professors Alan H. Barrett and Jerome B. Weisner, Sander Weinreb developed a one-bit correlator that enabled the Millstone antenna to look for evidence of the hydroxyl radical (OH) in outer space. In 1963, a successful measurement campaign was completed. The analysis confirming the existence of OH was the first time a molecule was detected in outer space [72].

Bernard Burke, MIT professor of physics, and Alan E.E. Rogers, a student of Barrett, began an interferometry program to measure characteristics of OH masers in space. This work started in 1965 with a modest baseline of 700 m between the Haystack and Millstone antennas. In 1966, James M. Moran, another student of Barrett, joined the team and extended the interferometry to a 13-km baseline between Millstone and the Harvard Agassiz antennas. Subsequent measurements employed a longer baseline between the Haystack antenna and the National Radio Astronomy Observatory, Green Bank, West Virginia. Following the success with bistatic operations, tests involving additional observatories at Hat Creek, California, and Onsala, Sweden, were performed to determine the size of the OH maser for the first time [73, 74].

Shapiro and Rogers also applied VLBI techniques to geodesy. This work led to accurate intercontinental measurements of tectonic-plate movement and earthquake fault lines. GPS measurements have since supplanted VLBI measurements of various geodetic

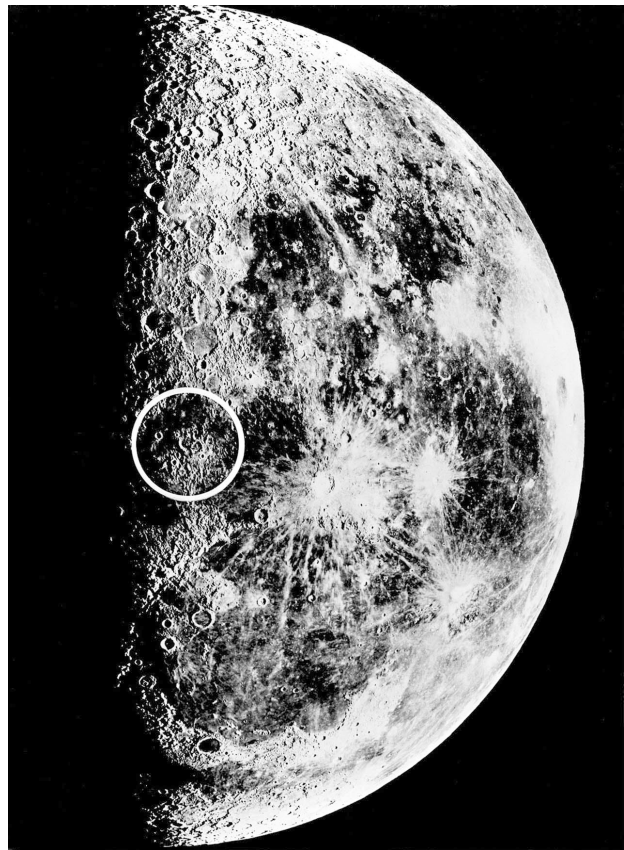


**FIGURE 16.** Footprint of the 8-GHz beam from the Haystack antenna on the surface of the Moon.

parameters. VLBI, however, continues to be the principal instrument for the measurement of the rotation of the Earth and polar motion [75–77].

#### *Lunar Studies*

In 1958, the Millstone UHF radar was the most powerful radar used up to that time to observe the Moon. Pettengill led an effort to confirm the quasi-specular returns seen by other radars and discovered weaker diffuse returns with strongly cross-polarized reflections [78]. (For more information on this topic, see the article entitled “Wideband Radar for Ballistic Missile Defense and Range-Doppler Imaging of Satellites,” by William W. Camp et al., in this issue.)

A bistatic Moon-bounce experiment was performed between a Stanford Research Institute transmitting site at College, Alaska, and receivers at the Canadian Defence Research Telecommunication Establishment, Shirley Bay, Ottawa, Ontario, and at Millstone to characterize auroral-propagation effects.

The principal legacy of the experiment was the analysis of the effects of the libration of the Moon on the spectral characteristics of lunar echoes [79, 80].

By the mid-1960s, radar measurements, together with subsequent measurements from other radars (including the Millstone L-band radar), were used to confirm the existence of a relatively smooth undulating lunar surface (with an average slope of  $\sim 11^\circ$ ) coupled with boulders strewn about to account for the diffuse returns [54, 56, 57]. The crater Tycho was characterized at 23 cm and later at 3.2-cm and 70-cm wavelengths [81, 82].

The narrow Haystack antenna beam pinpointed a spot 200 km in diameter centered on the apparent axis of the Moon (its libration axis) [83]. The small spot size, shown in Figure 16, made possible the resolution of the Doppler ambiguity that exists when using a radar beamwidth that exceeds the Moon's diameter. The Doppler ambiguity was resolved by mapping range-Doppler contours on the surface of a rotating sphere, as shown in Figure 17. Extensive analysis based on radar data overcame the accuracy

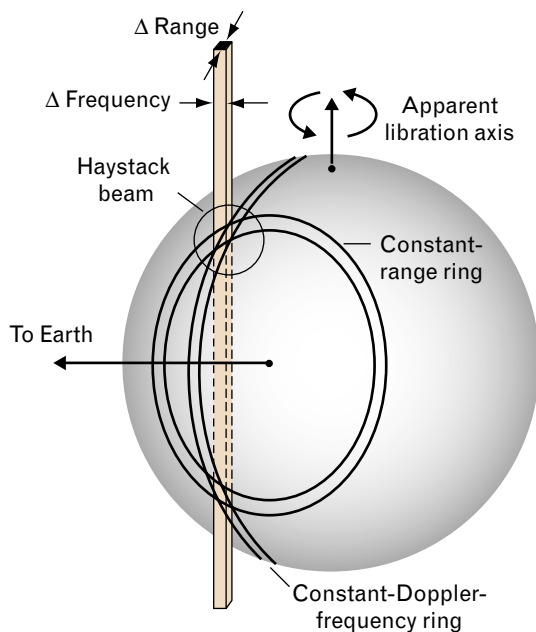


**FIGURE 17.** Projection of constant range and Doppler contours on the surface of the Moon. The projection of the narrow Haystack beam allows resolution of the ambiguity that exists in the intersection of the contours. The contours are referred to the apparent axis of rotation of the Moon relative to the observation point on the Earth (libration axis).

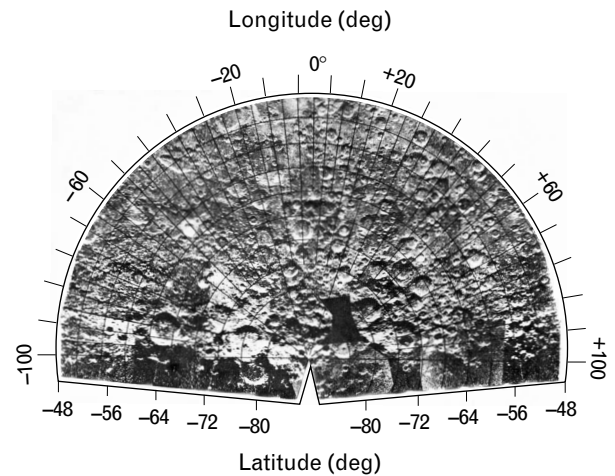


**FIGURE 18.** Mosaic radar map of the Moon from latitude  $48^\circ\text{S}$  to  $90^\circ\text{S}$  and longitude  $104^\circ\text{E}$  to  $104^\circ\text{W}$ . Approximately 120 individual areas were surveyed as the apparent axis of rotation of the Moon allowed the radar beam to be positioned unambiguously on the region of interest.

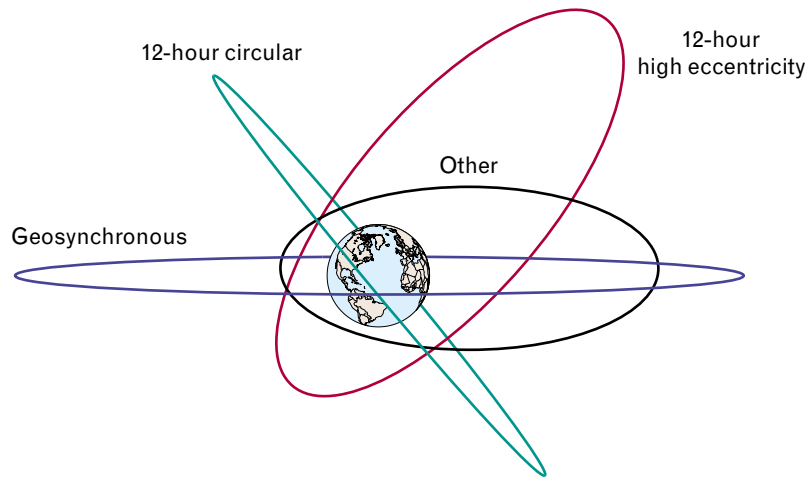
limitations in the published lunar ephemeris. Extensive radar data processing to obtain topography and albedo yielded a mosaic map of  $\sim 51\%$  of the Moon's surface. The resolution was comparable to or better than that from an optical telescope on Earth.

High-resolution maps of the Moon, such as the one shown in Figure 18, were made to convey details of local albedo [60]. These approximately  $2\text{-km} \times 2\text{-km}$ -resolution maps and the collateral data played a role in NASA's plans to put men on the Moon and collect geologic specimens. Stanley Zisk helped advise NASA in real time as astronauts selected specimens.

A great advantage of the Haystack mapping was the ability to resolve details at the limb of the Moon that could not be adequately imaged by optical means. Haystack was also useful in bringing the discrepancies between radar data and the lunar ephemeris to the attention of the astronomical community [61].

In the period from the end of the 1950s through the 1960s, Lincoln Laboratory scientists used the Millstone radar to make numerous important contributions to lunar, planetary, and ionospheric studies. By the end of the 1960s, Millstone's radar-astronomy usefulness was diminishing because of advances in other technology. But at this time, satellite detection and tracking for space surveillance was becoming an





Typical Orbital Parameters				
Orbit Class	Number of Objects	Mean Motion (revs/day)	Perigee (km)	Apogee (km)
12-hour circular	151	~2	15,000	25,000
12-hour high eccentricity	188	~2	<2000	>20,000
Geosynchronous	752	~1	30,000	42,000
Other	780	<6.5	—	>~5900

**FIGURE 21.** Distribution of the current resident space-object population (a total of 1871 objects as of August 2000), according to major classes of deep-space orbits. (Adapted from Reference 90.)

satellites at long ranges. By early 1975, in response to Air Force needs for improved timely tracking of deep-space objects, the Millstone radar again became a contributing sensor to the network, and it continues in that role to this day. Figure 20 includes a frame captured from a 1976 16-mm film of the Millstone real-time tracking display. The peak in the center results from the processing of 512 pulses and represents the signal from a target tracked at 19,000 km. This real-time FFT processing, coupled with real-time orbit propagation and a variety of search techniques, forms the foundation for the radar tracking of deep-space objects used today.

Since that time the techniques developed at Millstone have been the cornerstone of a network of radar sensors that track a dramatically increasing number of objects in deep-space orbit (formally designated by

Space Command as objects with orbits greater than a 225-min period) [89]. The current population of objects in deep-space orbits has grown to more than 1800 as the technology for communications, navigation, and surveillance has exploded. Figure 21 summarizes the orbital distribution of these objects.

The principal regimes of deep-space orbits include

1. 12-hr circular orbits—primarily populated by U.S. GPS satellites and the Russian GLONASS navigation satellites.
2. 12-hr high-eccentricity orbits—primarily populated by Russian Molniya communication satellites and related objects. The apogees of those objects are designed to be in the northern hemisphere to maximize the communication capability along a large extent of longitude at high-latitude ground sites.

3. geosynchronous orbits —24-hr orbits generally at low inclination along the equator to provide essentially Earth-fixed position for communications and other functions. This category includes objects in near geosynchronous orbits that are either rocket stages, which were used to boost payloads into this orbit, or dead payloads that were boosted out of geosynchronous orbit into so-called graveyard orbits either below or above strictly geosynchronous orbit.
4. other—this category includes a broad variety of objects with a large mix of orbital parameters. A large segment of this category includes spent rocket bodies and significant numbers of other objects from Cape Canaveral launches ( $\sim 28^\circ$  inclination) and Ariane launches from French Guiana ( $\sim 7^\circ$  inclination).

As of August 2000, the total number of objects in the deep-space catalog was 1871 [90]. Space surveillance of the truly geosynchronous objects from any location on the Earth's surface is constrained to only that portion of the geosynchronous belt which is visible from that site. In contrast, for low-altitude and the other nonsynchronous orbits, potential coverage by a surveillance site is primarily constrained only by the inclination of the orbit relative to the site's latitude. In these cases, the site location rotates with the Earth under the orbit, which results in regular access to the satellite orbit.

The estimated orbits of these objects are maintained by regular tracking with both radar and electro-optical systems. The current radar sites include, in addition to the Millstone radar, the AN/FPS-85 [91] radar at Eglin Air Force Base, Florida, and the ALTAIR radar [92] on the Kwajalein Atoll in the Marshall Islands. Both of these sensors were enhanced directly with the multi-pulse processing developed at Millstone to perform the deep-space tracking function. The AN/FPS-85 had been established primarily as a low-altitude-target space-surveillance sensor in the mid-1960s. Millstone personnel installed the multi-pulse coherent tracking at the AN/FPS-85 in the late 1980s to significantly extend its detection range. That deep-space mode complements the standard low-altitude surveillance fences of the radar that provide a large amount of data to the overall

space-surveillance system. The low-altitude fences of the AN/FPS-85 also generate significant tracking data on highly eccentric deep-space objects, whose orbits in many cases intercept that fence at detectable ranges.

The deep-space tracking capabilities of Millstone have also been replicated on the ALTAIR radar, located on the Kwajalein Atoll in the Marshall Islands. The ALTAIR radar was originally built in 1969 as an instrumentation radar as part of the Pacific Range Electromagnetic Signature Studies (PRESS). The radar is a dual-frequency radar operating at both VHF (155–162 MHz) and UHF (422 MHz.) The deep-space capability was installed as part of the UHF system in 1982 [92]. Figure 22 shows the Millstone Hill radar, and Figure 23 shows the ALTAIR radar on Kwajalein Atoll in the Marshall Islands.

The contributing radar sensors, Millstone and ALTAIR, provide a significant amount of deep-space tracking data over a large fraction of the geosynchronous belt. Table 1 summarizes some of the principal operating characteristics of the Millstone radar. Operating at L-band (1295 MHz), the high-power transmitter coupled to the 84-ft antenna results in a signal-to-noise ratio with a 1-msec pulse of 50 dB on a  $1\text{-m}^2$  (0 dBsm) space object at a range of 1000 km. With coherent processing of a large number of pulses ( $\sim 1000$ ), the radar sensitivity can be further improved by 30 dB to mitigate the range losses of 64 dB going from near-Earth 1000-km ranges to the 40,000-km range typical of geosynchronous distance. By utilizing the 1-MHz radar bandwidth, the Doppler information available from the FFT processing, and the monopulse error channels, the radar consistently produces positional data with the accuracy indicated in the Millstone operating characteristics.

With sensitivity similar to Millstone, ALTAIR also produces a large number of high-quality deep-space observations with the accuracy indicated in Table 2, which lists key operating characteristics. Since 1975, the Millstone radar has taken over five million observations while performing over 500,000 satellite tracks in support of Space Command. Operating for a larger number of hours ( $\sim 128$  hours per week), ALTAIR has produced more than 700,000 tracks in its deep-space mode.



**FIGURE 22.** The Millstone Hill radar in its current configuration in Westford, Massachusetts. Multipulse coherent processing techniques were developed at the Millstone site to enhance the radar’s effectiveness as a deep-space tracking sensor.

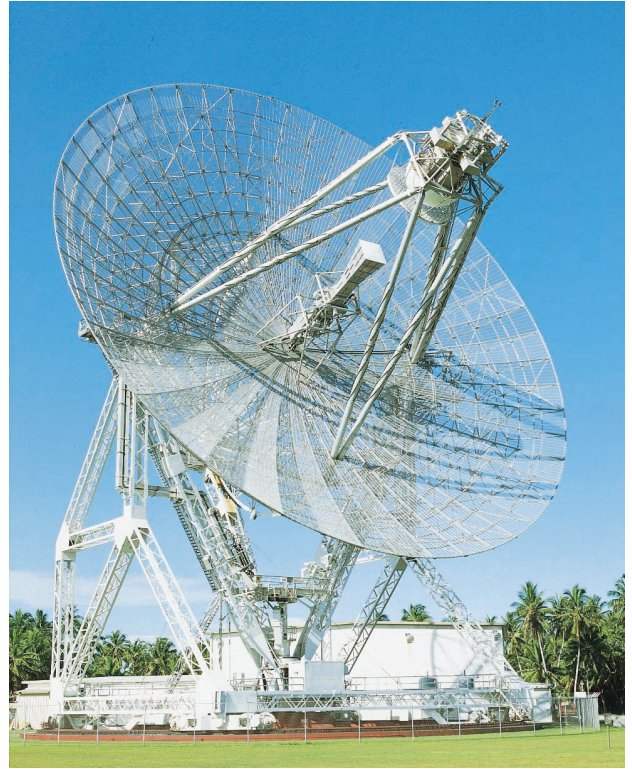


**FIGURE 23.** The ARPA Long-Range Tracking and Instrumentation Radar (ALTAIR) on Kwajalein Atoll in the Marshall Islands. Like the Millstone radar, ALTAIR is part of a network of contributing radar sensors that perform deep-space tracking.

**Table 1. Millstone Operating Characteristics**

Operating frequency	L-band (1295 MHz)
Dish	Steerable 84-ft dish
Beamwidth	0.6°
Peak power output	3 MW
Average power output	120 kW
Pulse-repetition frequency	40 Hz
Pulse length	1 msec
Signal-to-noise ratio (per pulse)	50 dB @ 1000 km (0-dBsm target)
<i>Accuracy</i>	
Range resolution	5 m
Range-rate resolution	5 mm/sec
Azimuth and elevation angle	0.01°

**Table 2. ALTAIR Operating Characteristics**

Operating frequency (deep-space mode)	UHF (422 MHz)
Dish	Steerable 150-ft dish
Beamwidth	1.1° (UHF)
Peak power output	5 MW
Average power output	120 kW
Pulse-repetition frequency	300 Hz
Pulse length	80 μsec
Signal-to-noise ratio (per pulse)	38 dB @ 1000 km (0-dBsm target)
<i>Accuracy</i>	
Range resolution	20 m
Range-rate resolution	15 mm/sec
Azimuth and elevation angle	0.03°

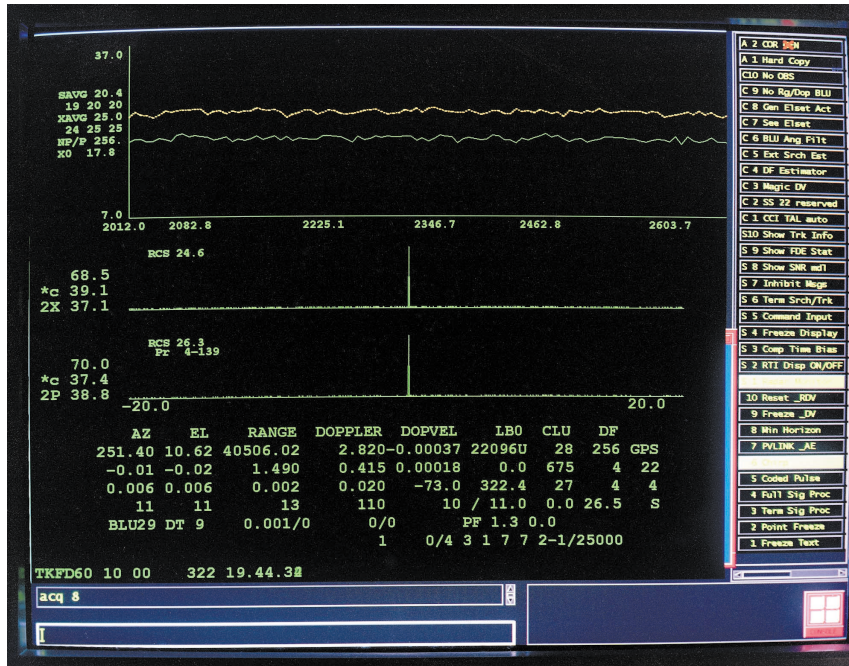


**FIGURE 24.** The Millstone real-time tracking display. The traces include results of FFT-based coherent integration for both polarizations and a recreated strip chart record (radar cross section versus time) at the top. Detailed status information is included at the bottom; operator tracking information is included along the right side.

The hardware components and operating details of the Millstone and ALTAIR radars in the deep-space modes are specific to each site, but they share the same fundamental characteristics. The remaining discussion focuses specifically on details of the Millstone system. Two Nighthawk computers perform the real-time processing of the system. These computers represent the fourth generation of computers used to drive the real-time tracking system for deep-space tracking.

The current real-time tracking system produces the tracking display shown in Figure 24. This display demonstrates the principal features of the tracking system. In this case, a geosynchronous satellite is being tracked at a range of 40,506 km from the radar. In the center of the screen are two FFT-based displays showing the results of processing 1024 (256 × 4) pulses for both the principal polarization (transmit right circular, receive left circular) channel on the bottom and orthogonal polarization (receive right circular) channel above. The radar-return signal from that target is the spike in each trace, and the relative signal strength in the principal polarization is only 1.5 dB

(70.0 versus 68.5) greater on the displayed scale than the orthogonal polarization. The topmost trace represents the signal/radar-cross-section history of the track and shows a steady radar cross-section of the satellite of close to 25 dBsm in the principal channel. The real-time display also includes a large amount of pointing and tracking status information below the display and the verification of a number of operator-selected modes along the right side.

On the basis of the Millstone tracking experience and the properties of the actual deep-space targets to be tracked, it has been found beneficial to utilize a variety of tracking modes to maximize tracking performance. The variety of the coherence properties of the objects, generally represented by the stability of payloads and the tumbling of uncontrolled objects and the polarization properties of the objects, has led to the development and installation of a sophisticated array of data-driven detection modes in the real-time tracking system. These modes are characterized in Figure 25.

The coherent target in the real-time tracking display of Figure 24 represents one possible coherency

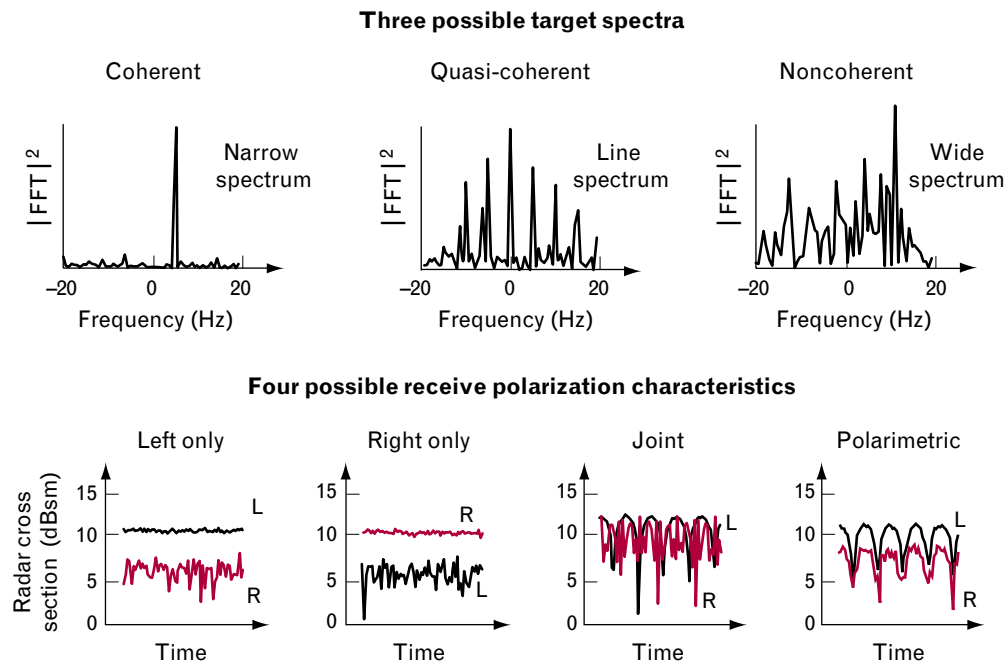


**FIGURE 25.** The upgraded Millstone data-driven processing system addressing the cases of three possible target-spectrum characteristics and four possible polarization characteristics. System performance is enhanced by simultaneously processing all of the possible combinations (twelve real-time processing models) and by using the strongest signal.

model. Figure 25 shows two other coherency models, a quasi-coherent model typified by a limited line-spectrum response on the FFT-amplitude scale, and a totally noncoherent model characterized by the spread of the response over a large fraction of the FFT sampling-bandwidth Doppler scale of the FFT. On the polarization axis of the target model, assuming right-circular transmission, examining both the left and right receive channels, four cases are possible: (1) left (principal) circular return only, (2) right (orthogonal) circular return only, (3) joint returns in both receive channels, and (4) polarimetric (i.e. correlated) returns in both channels.

Processing all possible models can improve the detection and tracking signal-to-noise ratio by several dB relative to much simpler versions, such as the single-polarization channel with coherent and noncoherent models, that were originally installed at the site. Additionally, processing all modes simultaneously and selecting the best model means that *a priori* target models are not required.

Another significant feature of deep-space tracking that has been developed and employed at Millstone is

the concept of sophisticated radar calibration [93]. To produce the highest quality metric data, the radar must achieve signal-to-noise-ratio-limited accuracy. In this case, errors introduced by atmospheric effects, inaccurate system biases, and changes in system performance must be monitored and accounted for. A necessary step in the calibration process is the determination of an independent standard that can be compared to actual site observations. Such a standard can be obtained from the orbits of several resident space objects, including the Laser Geodynamics Satellite (LAGEOS), that are derived from laser tracking of objects with laser retroreflectors. Tracking these objects with the radars, assuming a sufficient signal-to-noise ratio over a variety of antenna angles and atmospheric conditions, can determine system biases for the radars. These biases can be applied to the processing of the resulting data. Subsequently, regular tracking of these objects, particularly following any changes to the radar system, can be used to update and/or validate system biases. This technique has been used at Millstone for many years and that technology has now made the transition to support the

calibration of the entire Air Force tracking network.

The continued operation and upgrade of the Millstone radar as a contributing sensor has enabled the development of a number of processing techniques to improve the efficiency of the both the radar and the entire network. A continually upgraded set of automated tracking functions enables a single radar operator to simultaneously perform the tracking task, monitor system performance, and monitor the communications traffic. An advanced dynamic scheduling algorithm provides the operator with continuous updates to tracking priorities; these updates are based on satellite visibilities, tracking efficiency, and Air Force tasking requests. A suite of real-time and near-real-time orbit-determination software, both analytic and numerically based, has been developed to provide Space Command and other data users with the highest-quality positional data. Much of the technology developed in these processing systems has been transferred to other sites within the Space Surveillance Network.

The observations generated from tracking satellites at Millstone include independent measurements of range, range rate, azimuth, and elevation angle. Both the external and internal calibrations are used to maintain the one-sigma errors in these measurements to 5 m in range, 5 mm/sec in range rate, and  $0.01^\circ$  in both azimuth and elevation angle.

Once again, the confluence of radar technology development at Lincoln Laboratory and the emergence of a threat to national security spurred the development of a new capability. In 1972, the Soviet Union launched its first deep-space launch-detection satellite. This satellite was in an eccentric 12-hour orbit with an apogee height of about 40,000 km. The military use of both these and geosynchronous orbits posed a serious challenge to the United States. At the time, the country had no real-time capability to track satellites at these ranges, and relied on the development and analysis of films from a suite of Baker-Nunn cameras.

As in the ICBM case, Lincoln Laboratory had been doing research and experiments on the feasibility of using radars for the detection and tracking of the targets [86–88] in advance of a widespread recognition of the threat. In this case, the key technology devel-

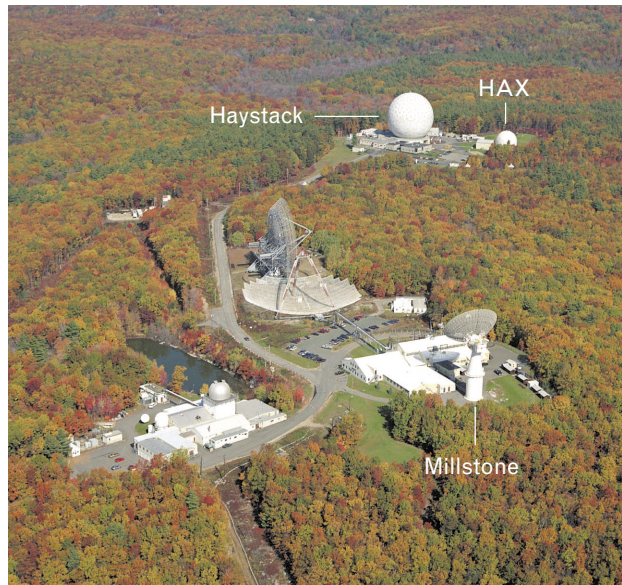


**FIGURE 26.** The Lincoln Laboratory Millstone Hill radar facility in Westford, Massachusetts. The Lincoln Space Surveillance Complex consists of the Millstone radar and the Haystack and Haystack Auxiliary (HAX) radars.

oped and applied at Millstone was the real-time coherent integration of many radar pulses over an extended period of time [87]. The coherence (i.e., stability) of the target return, the pulse-to-pulse coherence of the radar signal, and the use of Doppler processing to align a series of FFTs allowed many seconds of radar data (comprising echoes from tens of thousands of transmitted pulses) to be summed in real time to produce target returns sufficient for closed-loop tracking and real-time generation of positional data.

In 1995, the Millstone, Haystack, and Haystack Auxiliary (HAX) radars were organized to form the Lincoln Space Surveillance Complex (LSSC), shown in Figure 26. Radar operations are coordinated to synergistically support the objectives of metric tracking, satellite-launch coverage, and mission and payload assessment through range-Doppler imaging. An example is the use of Millstone with its  $0.6^\circ$  beamwidth to provide real-time pointing to Haystack ( $0.06^\circ$  beam) and HAX ( $0.1^\circ$  beam) for satellite acquisition. Another example is the use of narrowband cross-section measurements in conjunction with Haystack or HAX wideband data to assess such quantities as payload status and spin rate.

## Summary

Beginning in the mid-1950s and continuing today, Lincoln Laboratory has addressed a series of threats—ICBMs, near-earth satellites, and deep-space satellites—by designing, developing, and implementing high-power radar technology for surveillance. Many advances were made to provide both the theoretical underpinnings and the practical implementation. Among the key technologies developed were phase-coded pulse compression, Doppler processing, computer-guided tracking, range-Doppler imaging, and long-term coherent integration. The application of these technologies to lunar and planetary science established many of the foundational discoveries in this field.

Demonstration of capability was an integral part of system design and proved successful for both ballistic-missile early warning and deep-space satellite surveillance. The result of the tremendous effort and dedication by many talented people over the last four decades has been advances in the fundamental understanding of radars, the collection of surveillance data to meet critical national needs, and a legacy for future generations of radars.

## Acknowledgments

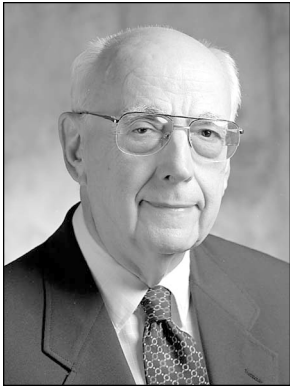
Paul B. Sebring established the environment in which engineers and scientists made effective contributions at the Millstone facility, beginning in 1957. He was also Lincoln Laboratory's first operational site manager at Kwajalein from 1962 to 1964. His leadership continued at the Millstone and Haystack facilities until 1979. The reestablishment of space-surveillance activities at Millstone in the mid-1970s owes much of its success to Antonio F. Pensa, currently a Lincoln Laboratory assistant director, whose leadership was instrumental in focusing the efforts of many talented staff members on the upgraded Millstone facility and, subsequently, on several other systems as well. Herbert G. Weiss was awarded the IEEE Aerospace and Electronic Systems Society 2000 Pioneer Award for his contributions to the development of the Millstone Hill and Haystack space surveillance radars. The authors also thank Alan Rogers, Joseph Salah, and Ramaswamy Sridharan for reviewing the article.

## REFERENCES

1. D.L. Clark, "Early Advances in Radar Technology for Aircraft Detection," in this issue.
2. K. Schaffel, *The Emerging Shield: The Air Force and the Evolution of Continental Air Defense, 1945–1960* (Office of Air Force History, Washington, 1990).
3. W.M. Siebert, "A Radar Detection Philosophy," *IRE Trans. Info. Theory* 2 (3), 1956, pp. 204–221.
4. W.M. Siebert, "The Development of AN/FPS-17 Coded-Pulse Radar at Lincoln Laboratory," *IEEE Trans. Aerosp. Electron. Syst.* 24 (6), 1988, pp. 833–837.
5. R.F. Lerner, "A Matched Filter Detection System for Complicated Doppler Shifted Signals," *IRE Trans. Info. Theory* 6 (3), 1960, pp. 373–385.
6. Pioneer Award Declaration for 1987, C.E. Cook and W.M. Siebert, *IEEE Trans. Aerosp. Electron. Syst.* 24 (6), 1988, p. 823.
7. G.H. Pettengill and D.E. Dustin, private communication.
8. K.S. Kelleher and H.H. Hibbs, "An Organ Pipe Scanner," Naval Research Laboratory Report 4141 (11 May 1953).
9. J.S. Arthur, J.C. Henry, G.H. Pettengill, and P.B. Sebring, "The Millstone Radar in Satellite and Missile Tracking," *Ballistic Missiles and Space Technology*, vol. III (Pergamon Press, New York, 1961), pp. 81–93.
10. R.C. Fritsch, "Antenna and RF Circuit Design Millstone Hill Radar," *Technical Report 193*, Lincoln Laboratory (7 Jan. 1959), DTIC #AD-658465.
11. W.H. Drury, W.F. Kelley, A.A. In, and D.R. Bromaghim, "Sequential Detection System for the Processing of Radar Returns," *Group Report 41G-0005*, Lincoln Laboratory (22 Mar. 1961), DTIC #AD-658465.
12. G.P. Dinneen, J.A. Dumanian, I.L. Lebow, I.S. Reed, and P.B. Sebring, private communications.
13. I. Shapiro, *The Prediction of Ballistic Missile Trajectories from Radar Observations* (McGraw-Hill, New York, 1958).
14. G.H. Pettengill and L.G. Kraft, Jr., "Observations Made with the Millstone Hill Radar," *Avionics Research: Satellites and Problems of Long Range Detection and Tracking, AGARD Avionics Panel Mtg., Copenhagen, 20–25 Oct. 1958*, pp. 125–134.
15. G.H. Pettengill, "A New Technique for Investigation of Meteor Echoes at UHF," *Geophys. Res. Lett.* 67 (1), 1962, pp. 409–411.
16. J.V. Evans and M. Loewenthal, "Ionospheric Backscatter Observations," *Planet. Space Sci.* 12, Oct. 1964, pp. 915–944.
17. J.V. Evans, "Radio-Echo Studies of Meteors at 68-Centimeter Wavelength," *J. Geophys. Res.* 70 (21), 1965, pp. 5395–5416.
18. E.N. Hayes, *Trackers of the Sky: A History of the Smithsonian Satellite-Tracking Program* (Howard A. Doyle Publishing, Cambridge, Mass., 1968).
19. J.V. Evans, W.A. Reid, and P. Stetson, "Upgrading Millstone Hill Radar for the International Magnetosphere Study," *National Science Foundation Final Report*, Lincoln Laboratory (1 Apr. 1978).
20. "Millstone Hill Observatory," vols. I and II, Lincoln Manual 51, Lincoln Laboratory (1 Apr. 1964).
21. C.A. Lindberg, "12-Horn Monopulse Antenna System for Millstone Radar," *Technical Report 393* (15 June 1965), DTIC #AD-627008.
22. L.J. Ricardi and L. Niro, "Design of a 12 Horn Monopulse Feed," *IRE Conv. Record, New York, 20–23 Mar. 1961*, pp. 49–56.

23. H.G. Weiss, "The Haystack Microwave Research Facility," *IEEE Spectr.* 2 (2), 1965, pp. 50–69.
24. IEEE Aerospace and Electronic Systems Society 2000 Pioneer Award for Development of the Millstone Hill and Haystack Space Surveillance Radars; presented to Herbert G. Weiss (Lincoln Laboratory), *IEEE Trans. Aerosp. Electron. Syst.* 37 (1), 2001, pp. 361–379.
25. J. Ruze, "Antenna Tolerance Theory—A Review," *Proc. IEEE* 54 (4), 1966, pp. 633–640.
26. A.O. Kuhnel, "Haystack Antenna System Status Report," *Technical Report 328*, Lincoln Laboratory (13 Sept. 1963), DTIC #AD-600930.
27. H. Simpson, "Structural Aspects of Large Precision Antennas," *NEREM Rec. 4, Boston, 5–7 Nov. 1962*, pp. 70, 197.
28. G.R. Carroll, "A Hydrostatic Bearing for Haystack," *ASME Winter Mtg., New York, 25–30 Nov. 1962*, paper no. 62-WA-299.
29. R.P. Ingalls, J. Antebi, J.A. Ball, R. Barvainis, J.F. Cannon, J.C. Carter, P.J. Charpentier, B.E. Corey, J.W. Crowley, K.A. Dudevoir, M.J. Gregory, F.W. Kan, S.M. Milner, A.E.E. Rogers, J.E. Salah, and M.S. Zarghamee, "Upgrading the Haystack Radio Telescope for Operation at 115 GHz," *Proc. IEEE* 82 (5), May 1994, pp. 742–755.
30. M.S. Zarghamee and J. Antebi, "Surface Deformation of Cassegrain Antennas," *IEEE Trans. Antennas Propag.* 33 (8), 1985, pp. 828–837.
31. R. Barvainis, J.A. Ball, R.P. Ingalls, and J.E. Salah, "The Haystack Observatory  $\lambda$ 3-mm Upgrade," *Publ. Astron. Soc. Pac.* 105 (693), 1993, pp. 1334–1341.
32. A.E.E. Rogers, R. Barvainis, P.J. Charpentier, and B.E. Corey, "Corrections for the Effects of a Radome on Antenna Surface Measurements by Microwave Holography," *IEEE Trans. Antennas Propag.* 41 (1), 1993, pp. 77–84.
33. C.W. Jones, "The Microwave System for the Haystack Planetary Radar," *Technical Report 457*, Lincoln Laboratory (23 Oct. 1968), DTIC #AD-685696.
34. P. Green and R. Price, private communications.
35. P.E. Green, "Radar Astronomy Measurement Techniques," *Technical Report 282*, Lincoln Laboratory (12 Dec. 1962), DTIC #AD-400563.
36. J.V. Evans and T. Hagfors, eds., *Radar Astronomy* (McGraw Hill, New York, 1968).
37. V.C. Pineo, L.G. Kraft, and H.W. Briscoe, "Ionospheric Backscatter Observation at 440 Mc/s," *J. Geophys. Res.* 65 (5), 1960 pp. 1620–1621.
38. V.C. Pineo and H.W. Briscoe, "Discussion of Incoherent Backscatter Power Measurements at 440 Mc/s," *J. Geophys. Res.* 66 (11), 1961, pp. 3965–3966.
39. W.E. Gordon, "Incoherent Scattering of Radio Waves by Free Electrons with Application to Space Exploration by Radar," *Proc. IRE* 46 (11), 1958, pp. 1824–1829.
40. J.V. Evans, J.M. Holt, and R.W. Wand, "On the Formation of Daytime Troughs in the F-Region within the Plasmasphere," *Geophys. Res. Lett.* 10 (5), 1983, pp. 405–408.
41. J.V. Evans and R.H. Wand, "Traveling Ionospheric Disturbances Detected by UHF Angle-of-Arrival Measurements," *J. Atmos. Terr. Phys.* 45 (4), 1983, pp. 255–265.
42. J.V. Evans, "Diurnal Variation of the Temperature of the F-Region," *J. Geophys. Res.* 67 (12), 1962, pp. 4914–4920.
43. J.V. Evans, "Ionospheric Temperatures during the Launch of NASA Rocket 8.14 on July 2, 1963," *J. Geophys. Res.* 69 (7), 1964, pp. 1436–1444.
44. J.V. Evans, "A Comparison of Rocket, Satellite, and Radar Determinations of Electron Temperature at Midlatitudes," *J. Geophys. Res.* 70 (17), 1965, pp. 4365–4374.
45. J.V. Evans, J.M. Holt, W.L. Oliver, and R.H. Wand, "Millstone Hill Incoherent Scatter Observations of Auroral Convection over  $60^\circ \leq \Lambda \leq 75^\circ$ ," *J. Geophys. Res.* 85 (A1), 1985, pp. 41–54.
46. J.V. Evans, ed., "Millstone Hill Radar Propagation," *Technical Report 509*, Bell Laboratories and Lincoln Laboratory (13 Nov. 1973), DTIC #AD-781179/7.
47. J.H. Ghiloni, "Millstone Radar Propagation Study: Instrumentation," *Technical Report 247*, Lincoln Laboratory (20 Sept. 1973), DTIC #AD-775140.
48. A. Gradisar, G. Schennum, J. Ruze, and M.L. Stone, "Development of a High Power Frequency Selective Cassegrain Sub-Reflector (FSS)," *G-AP Int. Symp., Columbus, Ohio, 14–16 Sept. 1970*, p. 407.
49. G.H. Schennum, "Frequency-Selective Surfaces for Multiple-Frequency Antennas," *Microw. J.* 16 (5), 1973, pp. 55–57, 76.
50. W.G. Abel and R.E. Newell, "Measurements of the Afternoon Radio Aurora at 1295 MHz," *J. Geophys. Res., Space Phys.* 74 (1), 1969, pp. 231–245.
51. A.J. Coster, "Use of GPS in Satellite Tracking: Real-Time Estimation of Ionospheric Refraction," *IAP '92 Technical Seminar Series, MIT, Cambridge, Mass., 14 Jan. 1992* [submitted].
52. A.J. Coster and M.J. Buosanto, "Comparison of Millstone Hill GPS and Incoherent Scatter Total Electron Content Measurements," *1992 Int. Beacon Satellite Symp., MIT, Cambridge, Mass., 6–10 July 1962*, pp. 113–117 [submitted].
53. J.W. Meyer, "Program Description—Radar Observations of the Planets," *Technical Note 1965-35* (9 July 1965), DTIC #AD-619708.
54. J.V. Evans and G.H. Pettengill, "The Scattering Properties of the Lunar Surface at Radio Wave Lengths," chap. 5 in *The Moon, Meteorites, and Comets (The Solar System)*, vol. IV, B.M. Middlehurst and G.P. Kuiper, eds. (University of Chicago Press, Chicago, 1963), pp. 129–161.
55. J.V. Evans and G.H. Pettengill, "The Radar Cross Section of the Moon," *J. Geophys. Res.* 68 (17), 1963, pp. 5098–5099.
56. J.V. Evans and T. Hagfors, "Study of Radio Echoes from the Moon at 23 Centimeters Wavelength," *J. Geophys. Res.* 71 (20), 1966, pp. 4871–4889.
57. J.V. Evans and T. Hagfors, "On the Interpretation of Radar Reflections from the Moon," *Icarus* 3 (2), 1964, pp. 151–160.
58. R. Price, P.E. Green, T.J. Goblick, Jr., R.H. Kingston, L.G. Kraft, Jr., R. Silver, and W.B. Smith, "Radar Echoes from Venus," *Science* 129 (3351), 1959, pp. 751–753.
59. G.H. Pettengill and R. Price, "Radar Echoes from Venus and a New Determination of the Solar Parallax," *Planet. Space Sci.* 5 (1), 1961, pp. 71–74.
60. G.H. Pettengill, "Radar Studies of the Moon: Final Report," Lincoln Laboratory (28 Feb. 1970).
61. C.R. Smith, G.H. Pettengill, I.I. Shapiro, and F.S. Weinstein, "Discrepancies between Radar Data and the Lunar Ephemeris," *Science* 160 (3830), 1968, pp. 876–878.
62. G.H. Pettengill, "Radar Studies of Mars: Final Report," Lincoln Laboratory (15 Feb. 1970).
63. A.E.E. Rogers, M.E. Ash, C.C. Counselman, I.I. Shapiro, and G.H. Pettengill, "Radar Measurements of the Surface Topography and Roughness of MARS," *Radio Sci.* 5 (2), 1970, pp. 465–473.
64. G.H. Pettengill, I.I. Shapiro, M.E. Ash, R.P. Ingalls, L.P. Rainville, W.B. Smith, and M.L. Stone, "Radar Observations of Icarus," *Icarus* 10 (3b), 1968, pp. 432–435.
65. L.B. Spence, private communications with G.P. Banner.
66. G.H. Pettengill, H.W. Briscoe, J.V. Evans, E. Gehrels, G.M.

- Hyde, L.G. Kraft, R. Price, and W.B. Smith, "A Radar Investigation of Venus," *Astron. J.* **67** (4), 1962, pp. 181–190.
67. M.E. Ash, I.I. Shapiro, and W.B. Smith, "Astronomical Constants and Planetary Ephemerides Deduced from Radar and Optical Observations," *Astron. J.* **72** (3), 1967, pp. 338–350.
  68. I.I. Shapiro, "Planetary Radar Astronomy," in *Moon and Planets* (North-Holland Publishing Co., Amsterdam, 1967), pp. 103–125.
  69. G.H. Pettengill, C.C. Counselman, L.P. Rainville, and I.I. Shapiro, "Radar Measurements of Martian Topography," *Astron. J.* **74** (3), 1969, pp. 461–482.
  70. I.I. Shapiro, G.H. Pettengill, M.E. Ash, M.L. Stone, W.B. Smith, R.P. Ingalls, and R.A. Brockelman, "Fourth Test of General Relativity: Preliminary Results," *Phys. Rev. Lett.* **20** (22), 1968, pp. 1265–1269.
  71. I.I. Shapiro, "Radar Determination of the Astronomical Unit," *Proc. Int. Astronomy Union, Paris, 20 Sept. 1965*, pp. 177–215 [submitted].
  72. S. Weinreb, A.H. Barrett, M.L. Meeks, and J.C. Henry, "Radio Observations of OH in the Interstellar Medium," *Nature* **200** (4909), 1963, pp. 829–831.
  73. H.F. Hinteregger, "A Long Baseline Interferometer System with Extended Bandwidth," *NEREM Record 1968, Boston, 6–8 1968*, pp. 66–67.
  74. A.E.E. Rogers, "Very Long Baseline Interferometry with Large Effective Bandwidth for Phase-Delay Measurements," *Radio Sci.* **5** (10), 1970, pp. 1239–1247.
  75. I.I. Shapiro and C.A. Knight, "Geophysical Applications of Long-Baseline Radio Interferometry," in *Earthquake Displacement Fields and the Rotation of the Earth*, L. Mansinha, D.E. Smylie, and A.E. Beck, eds. (Springer-Verlag, New York, 1970), pp. 284–301.
  76. I.I. Shapiro, D.S. Robertson, C.A. Knight, C.C. Counselman III, A.E.E. Rogers, H.F. Hinteregger, S. Lippincott, A.R. Whitney, T.A. Clark, A.E. Niell, and D.J. Spitzmesser, "Transcontinental Baselines and the Rotation of the Earth Measured by Radio Interferometry," *Science* **186** (4167), 1974, pp. 920–922.
  77. T.A. Herring, I.I. Shapiro, T.A. Clark, C. Ma, J.W. Ryan, B.R. Schupler, C.A. Knight, G. Lundqvist, D.B. Shaffer, N.R. Vandenberg, B.E. Corey, H.F. Hinteregger, A.E.E. Rogers, J.C. Webber, A.R. Whitney, G. Elgered, B.O. Ronnang, and J.L. Davis, "Geodesy by Radio Interferometry: Evidence for Contemporary Plate Motion," *J. Geophys. Res.* **91** (B8), 1986, pp. 8341–8347.
  78. G.H. Pettengill, "Measurements of Lunar Reflectivity Using the Millstone Radar," *Proc. IRE* **48** (5), 1960, pp. 933–934.
  79. S.J. Fricker, "Comparison of Measured and Computed Values of the Rapid Fading-Rate of Ultra High-Frequency Signals Reflected from the Moon," *Nature* (London) **182**, 22 Nov. 1958, pp. 1438–1439.
  80. J.C. James, L.E. Bird, R.P. Ingalls, M.L. Stone, J.W.B. Day, G.E.K. Lockwood, and R.I. Presnell, "Observed Characteristics of an Ultra-High-Frequency Signal Traversing an Auroral Disturbance," *Nature* **185** (4172), 1960, pp. 510–512.
  81. G.H. Pettengill and J.C. Henry, "Enhancement of Radar Reflectivity Associated with the Lunar Crater Tycho," *J. Geophys. Res.* **67** (12), pp. 4881–4885.
  82. G.H. Pettengill and T.W. Thompson, "A Radar Study of the Lunar Crater Tycho at 3.8-cm and 70-cm Wavelengths," *Icarus* **8** (3), 1968, pp. 457–471.
  83. J.V. Evans and T. Hagfors, "Radar Studies of the Moon," in *Advances in Astronomy and Astrophysics*, vol. 8, Z. Kopal, ed. (Academic Press, London, U.K., 1971), pp. 29–106.
  84. G.H. Pettengill and L.G. Kraft, Jr., "Earth Satellite Observations Made with the Millstone Hill Radar," *AGARD Avionics Panel Mtg., Copenhagen, 20–25 Oct. 1958*, pp. 125–134.
  85. R.R. Silva, private communications.
  86. G.L. Guernsey and C.B. Slade, "Observations of a Synchronous Satellite with the Haystack Radar," *Technical Note 1972-41*, Lincoln Laboratory (13 Dec. 1972), DTIC #AD-754937.
  87. G.P. Banner, private communications.
  88. L.B. Spence, A.F. Pensa, and T.E. Clark, "Radar Observations of the IMP-6 Spacecraft at Very Long Range," *Proc. IEEE* **62** (12), 1974, pp. 1717–1718.
  89. A.F. Pensa and R. Sridharan, private communications with G.P. Banner.
  90. NASA Goddard Satellite Situation Report, Aug. 2000, <<http://oig1.gsfc.nasa.gov>>.
  91. *Jane's Radar and Electronic Warfare Systems, 2000–2001*, M. Streeby, ed. (Jane's Information Group, Coulsdon, Surrey, U.K., 2000).
  92. K.R. Roth, M.E. Austin, D.J. Frediani, G.H. Knittel, and A.V. Mrstik, "The Kiernan Reentry Measurements System on Kwajalein Atoll," *Linc. Lab. J.* **2** (2), 1989, pp. 247–276.
  93. E.M. Gaposchkin and A.J. Coster, "Analysis of Satellite Drag," *Linc. Lab. J.* **1** (2), 1988, pp. 203–224.



**MELVIN L. STONE** is a senior staff member in the Air Traffic Control Systems group, which develops technology for monitoring and controlling aircraft operations. Mel received an S.B. in electrical engineering from MIT in 1951. He participated in the development of weather-radar techniques as a member of the staff of the MIT Department of Meteorology Weather Radar Laboratory from 1948 to 1951. Since he joined Lincoln Laboratory, forty years ago, his research interests have included weather radar, HF ground-wave radar, the lunar albedo at UHF, auroral backscatter and propagation effects related to ballistic missile defense, and the perturbation of the ionosphere caused by missile exhaust. He played a key role in system engineering during the construction of the Haystack radar facility and in the development of the 500-kW average power, X-band radar used in the fourth test of general relativity. Mel was the leader of the group responsible for testing and demonstration of the developmental air-to-ground radar that employed the displaced phase center concept. This radar was the progenitor of the U.S. Air Force/Army Joint Standoff Target Attack Radar System (Joint STARS). He serves as a consultant to the Federal Aviation Administration on radar systems for aircraft and weather surveillance. He is a member of the IEEE, the American Geophysical Union, Sigma Xi, and Eta Kappa Nu.



**GERALD T. BANNER** received S.B., S.M., and E.E. degrees from MIT before joining MIT Lincoln Laboratory in 1972. He is currently the leader of the Space Control Systems group, which focuses on the development of systems and techniques primarily addressing space-surveillance applications. That effort involves deep-space radars at Millstone Hill, electro-optics sensors, and the operational demonstration of an orbiting Space-Based Visible (SBV) sensor for space-surveillance applications. Previously he was a principal in the development of the Millstone Hill radar as the first deep-space tracking radar and a contributor to the establishment of the Experimental Test System (ETS) as a prototype for ground-based electro-optical space-surveillance system (GEODSS). He has also been a participant in several campaigns and studies related to the measurement and estimation of space debris. Recently he has been involved in several studies addressing the architecture of future space-surveillance systems. He is a member of the IEEE, Tau Beta Pi, and Eta Kappa Nu.